Hindawi Publishing Corporation
Journal of Sensors
Volume 2016, Article ID 3816094, 31 pages
http://dx.doi.org/10.1155/2016/3816094

Review Article

In_2O_3- and SnO_2-Based Thin Film Ozone Sensors: Fundamentals

G. Korotcenkov,[1] V. Brinzari,[2] and B. K. Cho[1]

[1]*Gwangju Institute of Science and Technology, Gwangju 500-712, Republic of Korea*
[2]*State University of Moldova, 2009 Chisinau, Moldova*

Correspondence should be addressed to G. Korotcenkov; ghkoro@yahoo.com and B. K. Cho; chobk@gist.ac.kr

Received 22 December 2015; Accepted 11 February 2016

Academic Editor: Eduard Llobet

The paper considers SnO_2 and In_2O_3 thin films as materials for the design of solid-state conductometric ozone sensors in depth. In particular, the present review covers the analysis of the fundamentals of SnO_2- and In_2O_3-based conductometric ozone sensor operation. The main focus is on the description of mechanisms of ozone interaction with metal oxides, the influence of air humidity on sensor response, and processes that control the kinetics of sensor response to ozone.

1. Introduction

Ozone is a highly reactive form of oxygen. The molecules of ozone contain three oxygen atoms (O_3) and are unstable with respect to O_2. A certain amount of ozone is produced in the troposphere in a chain of chemical reactions involving hydrocarbons and nitrogen-containing gases. Though ozone is a minor atmospheric constituent, with an average concentration of about 3 ppmv (parts per million volume), this gas plays great role in our life. The ozone layer protects life on Earth from ultraviolet solar radiation and is a significant contributor to the radiative energy balance of the atmosphere. Most of the atmospheric ozone (90%) is located in the stratosphere with a maximum concentration between 17 and 25 km. This means that ground concentration of ozone is considerably smaller than in the stratosphere. However, this situation started to change during last decades. The increased level of ozone in the atmosphere is a result from the interaction between sunlight and various chemicals emitted into the environment by industrial means. Automobiles can significantly affect ozone measurements as well. The oxides of nitrogen emissions can be catalyzed by the summer sun, resulting in ozone alerts. Thus, ozone near the ground is a product of industrial and urban pollution. In addition, in the last decade, considerable interest was shown in ecologically clean "ozone" technologies [1–3] (see also http://www.io3a.org/ and http://www.ioa-ea3g.org/). It was established that ozone can be widely used in medicine, as well as in different technological processes [4–10]. Due to its special characteristics, ozone can be applied in industries such as pharmaceuticals, food, textiles, and chemicals, as well as in water preparation, medical treatment, deodorizing, and the purification of gases (Figure 1). For example, ozonation, which is an effective technique for sanitizing ultrapure water and treatment systems, was introduced in the semiconductor industry over 30 years ago. Unlike other agents, such as chlorine or chromic acid, ozone oxidation is not accompanied by the appearance of toxic waste, since this process generates only oxidation products and oxygen. Ozone can be used for the improvement of organoleptic qualities, bleaching, iron and manganese elimination from water, the reduction of organic substances in suspensions, and the elimination of toxic compounds. Because of its relatively short half-life, ozone is always generated on-site by ozone generators, which usually use UV light and corona discharge for ozone generation.

However, it has been established that high concentrations of this powerful oxidizing gas in the ambient atmosphere are hazardous to human health [11–13]. A high level of ozone gas in the atmosphere is harmful to the human respiratory system, causing inflammation and congestion of the respiratory tract. An individual who remains in a 0.1 ppm O_3 environment for two hours will sustain a loss of 20% breathing capacity and, after remaining in 1 ppm O_3 for six hours, will suffer an attack of bronchitis. A mouse kept in 10 ppm O_3 will not survive. It is necessary to note that

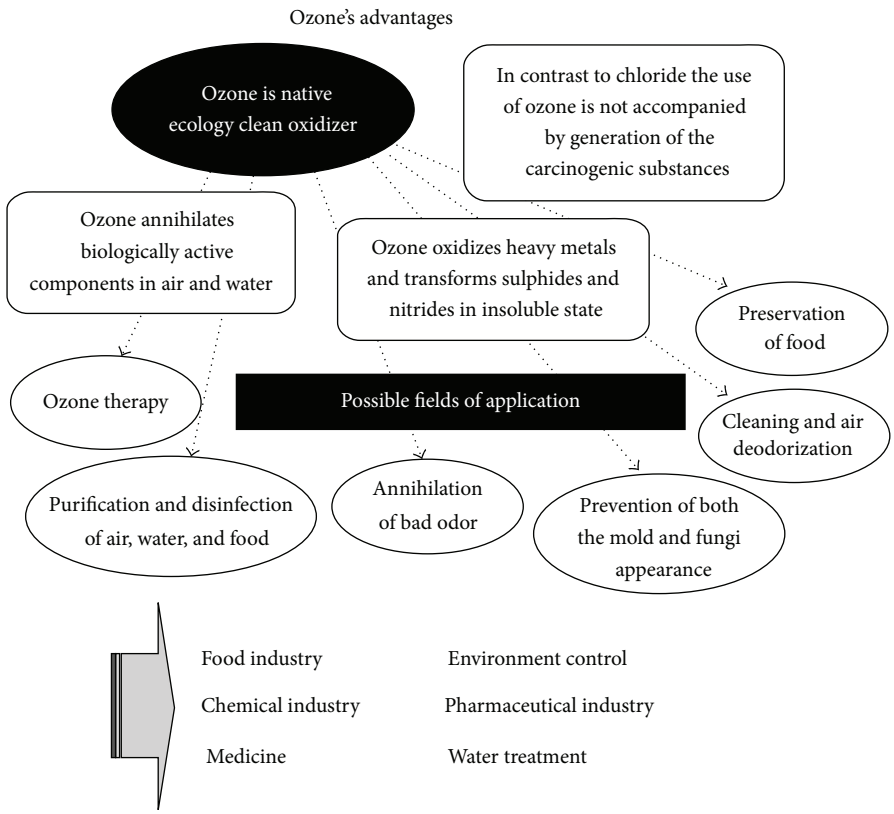

Figure 1: Advantages and possible fields of ozone applications.

ozone, due to its relatively short half-life (minutes in confined spaces), does not instantly diffuse in air to create a uniform concentration for easy measurement. Therefore, in order to control the ozone concentration in the atmosphere and surrounding environment, it is necessary to develop both effective and economical methods and devices for the continuous monitoring of ozone concentrations at multiple locations, including technological processes with incorporated ozone treatments. These methods are also needed to determine attenuation of the ozone layer by man-made gases, to validate model estimations of changes in ozone layer, and to confirm the efficiency of the Montreal Protocol on Substances that deplete the ozone Layer (http://ozone.unep.org/pdfs/Montreal-Protocol2000.pdf). As is well known, in recent decades there has been the depletion of the ozone layer, which can negatively affect the life on Earth. The increase in the number of articles devoted to the development and research of ozone sensors (see Figure 2) confirms the importance of this issue. Experiments have shown that analytical techniques developed to solve these problems should be capable of measuring ozone concentrations in the range of 0.01–10 ppm for these purposes. For example, ambient air measuring at the ground requires instruments with little ppb accuracy in a range 20–200 ppb, whereas in industrial and commercial applications the precision is not so stringent and the expected concentrations are higher (up to 10 ppm).

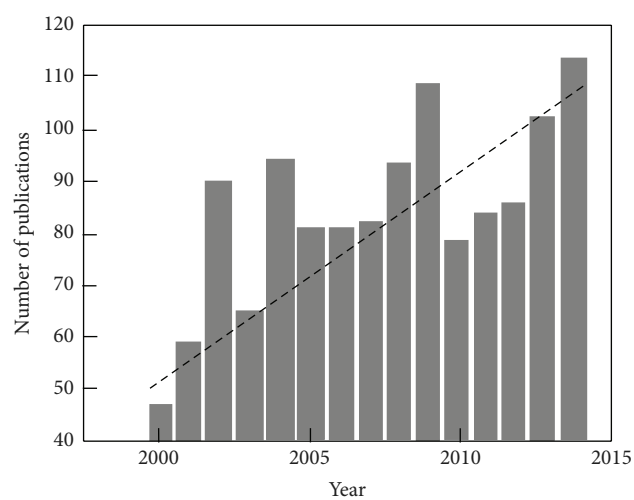

Figure 2: The growth in the number of publications devoted to the design of ozone sensors. Data extracted from Scopus.

At present, a number of conventional analytical methods, such as UV absorbance, optochemical, optical, chemiluminescence, fluorescence, and electrochemical methods, are available for the accurate analysis of ozone concentration in the air [14–17]. However, these sophisticated high accuracy techniques are advisable for application in both metropolitan

Table 1: Comparison of main types of sensors, which can be used for ozone detection.

Type of sensors	Detection limit, ppb	Advantages	Disadvantages
Optical: *UV absorbance* *UV-LIDAR technique*	1–30 20–200	Absolute measurements; reliability; RT operation; good selectivity; high accuracy; quick response; high resolution, high measuring range; long life time; acceptable for stationary instruments	Need UV source; interference from some organics and mercury; rather large size; fairly expensive per unit. This makes it very difficult if not impossible to design cheap portable device for in situ monitoring, in real-time distribution of ozone concentrations within large geographic areas
Optochemical: *chemiluminescence, fluorescence*	7–10	High sensitivity; RT operation	Need fuel and light source; fairly expensive per unit; the broadband character of luminescence spectra as well as the ubiquitous presence of naturally fluorescent compounds leads luminescence sensors to suffer from a critical lack of selectivity; sensitive to temperature fluctuations and other environmental factors that quench fluorescence
Electrochemical	50–100	Low-power consumption; RT operation; response is relatively quick; high accuracy; monitoring is continuous; high sensitivity; inexpensive and compact device acceptable for portable and fixed instruments	Less selective than optical technologies; sensitive to toxic gases and oxygen; have limitations in conditions of exploitation (temperature, pressure, and humidity); short life time at high concentration of ozone; drift is possible; need calibration; not fail-safe
Chemical: *chemical titration, diffusive and pumped ozone badges*	20–200	Inexpensive; simple; easy to use; RT operation	Low sensitivity; it is not selective; it is not a continuous monitoring process; tapes have limited life span and must be stored properly in control conditions
Polymer-based	>1000	Small size; RT operation; low consumable power; good sensitivity; acceptable for portable instruments	Commonly not selective; some polymers react strongly to water vapor; degradation under UV irradiation and ozone influence; drift is possible; need regular calibration
Conductometric metal oxide (MeOx) heated	5–10	High sensitivity to ozone; fast response; low-cost; robust; small size; wide operating temperature range; resistant to corrosive environments; long operating life; compact and durable; acceptable for portable instruments	Commonly not selective; drift of operating characteristics is possible; need regular calibration; nonlinear response; need oxygen; high enough power consumption; not fail-safe

and industrial urban areas under conditions of relatively high atmospheric pollutant concentration that are close to WHO guidelines. Moreover, as a rule, these methods are based on periodic air sampling and analysis of the samples with rather large and expensive stationary analytical devices. Therefore, it is very difficult, or even impossible, to track the distribution of ozone concentrations within large geographic areas in real time. In addition, the conventional analytical methods do not provide enough sensitivity for the detection of small concentrations of ozone in many cases [14, 16]. Solid-state conductometric gas sensors discussed in the present paper were designed especially for these purposes. Results of comparative analysis of the methods used for ozone monitoring are shown in Table 1.

2. Solid-State Conductometric Gas Sensors

The main advantages of solid-state conductometric gas sensors are ease of fabrication by using thin and thick film technologies, simple operation, and low production costs, because the materials and manufacturing techniques easily lend themselves to batch fabrication [18]. This means that well-engineered metal oxide conductometric sensors can be mass-produced at a reasonable cost. Reversibility, rapid response, longevity, and robustness are other merits of metal oxide gas sensors. Moreover, these sensors are compact and durable; therefore, they have very good suitability for the design of portable devices [18, 19]. This compensates for their disadvantages, such as low selectivity and temporal drift, and opens great opportunities for using them in alarm systems and portable instruments, including devices for balloon-borne atmospheric O_3 profile-sounding [20], electronic noises [21, 22], and sensor networks for air pollution monitoring with wireless communication [23]. Thus, compared to the reference methods discussed in the previous section, the use of low-cost conductometric ozone sensors for monitoring ambient air and technological processes would reduce air pollution monitoring costs and would also allow

Table 2: Conductometric-type ozone sensors and sensing materials used for their design.

Sensor type or principle of operation	T_{oper}, °C	Sensing materials
Pseudo-Schottky diode	RT–100	Pd (15 nm)/Ge (20 nm)/Pd (45 nm) on the p-type InP
Conductometric MeOx (heated)	200–400	In_2O_3; WO_3; SnO_2; ZnO; MoO_3-In_2O_3; In_2O_3-ZnO-SnO_2; ITO; NiO; $SmFeO_3$; Ga_2O_3/In_2O_3
RT conductometric MeOx	RT	$CuCrO_2$; $CuAlO_2$; In_2O_3:ZnO:SnO_2; SnO_2-In_2O_3
Conductometric MeOx (UV photoreduction/reoxidation)	RT	In_2O_3; ZnO; Pt/TiO_2-SnO_2
Conductometric MeOx (UV assistance)	RT	In_2O_3; SnO_2/SWNTs
Conductometric (polymer-based)	RT–150	Copper phthalocyanine (CuPc); polypyrrole (PPy); InAcAc
Conductometric (I-D structures)	RT–300	Carbon nanotubes network; In_2O_3; ZnO; SnO_2

larger spatial coverage especially in remote areas where monitoring with traditional facilities is cumbersome. One should note that solid-state conductometric gas sensors can be also used for controlling ozone concentration in water. They can take advantage of the gas permeability of polymer or another suitable membrane to separate the heart of the sensor from the water. This separation enables providing a controlled environment for sensor operation, while allowing ozone to enter from the sample and react with metal oxide surface. General descriptions of conductometric gas sensor fabrication and operation can be found in review papers [18, 24–32].

As shown in Table 2, at present, many materials [15, 32–41] have been tested for the design of conductometric ozone sensors, and many various technologies, such as sol-gel [42], laser ablation [35], sputtering [38], spray pyrolysis [43–45], RGTO [46], successive ionic layer deposition [47], vacuum evaporation [48], and solvothermal synthesis [49], have been applied for preparing gas-sensing layers based on these materials. Comparative evaluation of developed conductometric ozone sensors based on various metal oxides is shown in Table 3. It is seen that many of the above sensors have parameters suitable for practical use. However, in our survey we analyze conductometric ozone sensors designed on the base of SnO_2 and In_2O_3 thin films.

2.1. Advantages of In_2O_3 and SnO_2 for Ozone Sensor Design. One should note that the first ozone sensors based on the oxides mentioned above were designed by Takada et al. [76, 77] at the end of the 80s. SnO_2 and In_2O_3 are wide-band-gap semiconductors, which typically crystallize in the rutile and cubic structures correspondingly, and they are by far the most studied and most successful semiconductor materials for gas sensors [19], including development of ozone sensors (see Figure 3). These sensing materials have advantages, such as high sensitivity, fast response, and good thermal and temporal stability. Furthermore, In_2O_3- and SnO_2-based ozone sensors also show very low cross sensitivity. An experiment has shown that sensitivity to O_3, even in the ppb range, was much larger than the response to NO_2, CO, H_2, SO_2, and NH_3 in the tens of ppm range. In_2O_3 and SnO_2 also provide the opportunity for miniaturization and integration at micromachined substrates [14].

In_2O_3 and SnO_2 are gas-sensing materials, since they are conductive and possess the ability to donate electron density to the adsorbed oxygen molecules, which arises primarily due to bulk nonstoichiometry firstly within the oxygen lattice. Of course, the reactivity of the metal oxide surface is critically dependent on its doping, the defect structure, and the operating temperature. Possible oxygen anion states of adsorbed oxygen at the surface of SnO_2 and their transformations can be presented by the following scheme:

$$O_2\,(g) \longleftrightarrow O_2\,(ad) \overset{e^-}{\longleftrightarrow} O_2^{-}\,(ad) \overset{V_O}{\longleftrightarrow} O^{-}\,(ad) \overset{e^-}{\longleftrightarrow} O^{2-}\,(ad) \longleftrightarrow O^{2-}\,(lat) \tag{1}$$

In this scheme, (g) is gas, (ad) is adsorbed, and (lat) is lattice. All these transformations are thermally activated processes and as a rule are accompanied by charge transfer between adsorbed species and the conduction band of metal oxides (see Figure 4) [24, 78, 79]. Thus, the gas-sensing effect strongly points to an intrinsic defect reaction, such as oxygen vacancy (V_O) or the cation interstitial (Sn_i, In_i) mechanism [80]. As applied to the tin dioxide, these reactions can be described by the following schemes:

$$O \rightleftharpoons V_O^{2+} + \frac{1}{2}O_2 + 2e^- \tag{2}$$

$$Sn \rightleftharpoons Sn_i^{4+} + 4e^- \tag{3}$$

Table 3: The best parameters of conductometric heated ozone sensors designed on the base of metal oxides.

	Technological route, parameters of sensing layer	Max. sensor response	Conditions of measurements	Response time	Recovery times	References
In_2O_3	Thick film: d~100 nm, t~12 nm	$\sim 3 \cdot 10^2$	85°C, 250 ppb, dry	25–45 s	n/a	[35]
	Thick film: d—n/a, t~8 nm	$\sim 1.5 \cdot 10^3$	300°C, 100 ppb, dry	~1 min	~10 min	[50, 51]
	Thick film: d—n/a, t~8 nm	$\sim (4–6) \cdot 10^3$	350°C, 76 ppb	n/a	n/a	[33]
	Thick film: d~20 μm, t~20 nm	120	270°C, 1 ppm, dry	n/a	n/a	[52]
	Thin films: d~30–50 nm, t~10–15 nm	10^3–10^4	200–300°C, 1 ppm	<2 s (280°C)	~20 s (280°C)	[43, 44, 53, 54]
	Thin films: d—n/a, t—n/a	$\sim 10^2$	400°C, 60 ppb	100 min (250°C)	60–80 min (250°C)	[46]
	Thin films: d—n/a, t—n/a	$\sim 3 \cdot 10^2$	370°C, 230 ppb	n/a	n/a	[55]
SnO_2	Thick film: d~100 nm, t~15 nm	$\sim (3\text{-}4) \cdot 10^2$	120°C, 250 ppb, dry	40–60 s	Tens of minutes	[35]
	Thin films: d~30–50 nm, t~10–15 nm	10^3–10^4	200–300°C, 1 ppm	<2 s (280°C)	~15 min (280°C)	[45, 56, 57]
	Thin films: d~260 nm, t—n/a	$\sim 10^2$	350°C, 135 ppb	Several minutes	Several minutes	[58, 59]
	Thin films: d~300 nm, t—n/a	~10	350°C, 60 ppb	n/a	n/a	[60, 61]
	Thin films: d~20–30 nm, t~6–8 nm	$\sim 10^3$	320°C, 1 ppm	<2-3 s	~15 min	[47]
	Thin films: d~40–50 nm, t < 6–8 nm	$\sim 10^5$	150°C, 1 ppm	3-4 s (200°C)	~17 min (200°C)	[62]
WO_3	Thick film: d—n/a, t~15 nm	~600	180°C, 1 ppm	~15 s	~2 min	[35]
	Thick film: d—n/a, t—n/a	~35	400°C, 80 ppb	n/a	n/a	[63]
	Thin films: d~100 nm, t—n/a	$\sim 6 \cdot 10^2$–$7 \cdot 10^3$	120°C, 90 ppb	~12 s	1–3 min	[64]
	Thin films: d~35–50 nm, t~20–100 nm	5–300	250°C, 0.8 ppm	0.5–2 min	2-3 min	[65–69]
	Thin films: d~300 nm, t—n/a	~20	300°C, 200 ppb	Minutes	Minutes	[63]
	Thin films: d—n/a, t~20 nm	$1.5 \cdot 10^3$	300°C, 500 ppb	n/a	n/a	[70]
ZnO	Thick film: d—n/a, t~160 nm	~8	250°C, 0.1 ppm	14 s	9 s	[71]
	Thick film: d~275 nm, t—n/a	~10–30	200°C, 300 ppb	~10 s	~2 min	[72]
MoO_3-TiO_2	Thick film: d—n/a, t—n/a	1.7	370°C, 100 ppb	~20 s	n/a	[73]
Fe_2O_3	Thin films: d ~500 nm, t—n/a	~20	200°C, 0.5 ppm, 50%	n/a	n/a	[74]
$SmFeO_3$	Thick film: d—n/a, t—n/a	$\sim 10^2$	285°C, 0.4 ppm	~1 min	~10 min	[75]

d: film thickness; t: grain size; sensor response (R_{ozone}/R_{air}); conditions of measurements: temperature of operation, gas concentration, and humidity.

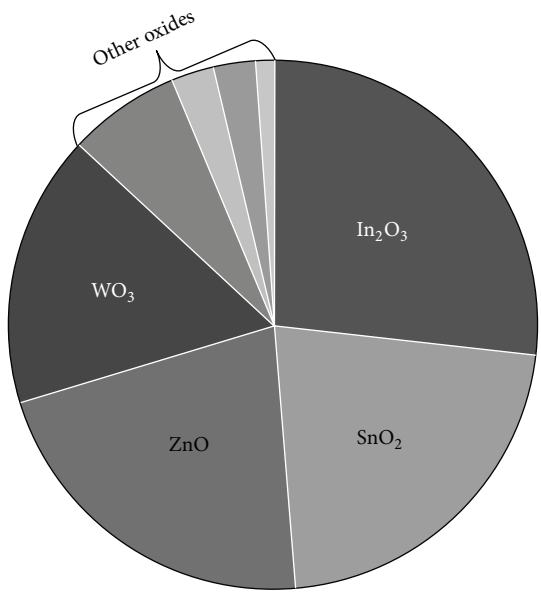

Figure 3: The percentage distribution of the number of articles devoted to the study of metal oxide-based ozone sensors. Data extracted from Scopus.

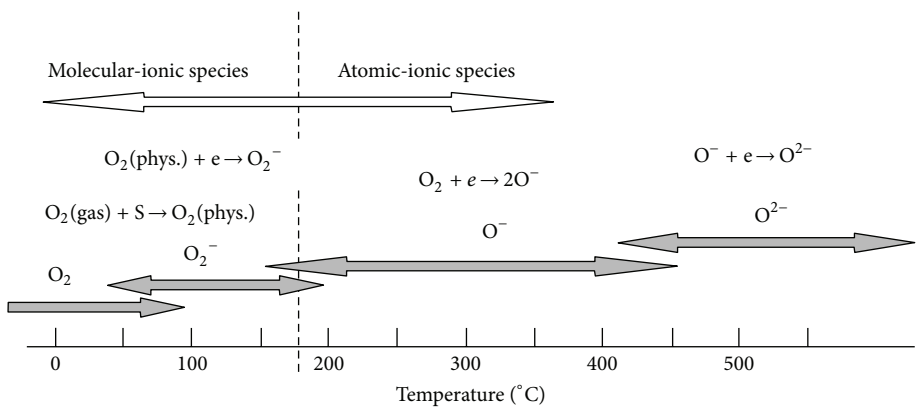

Figure 4: Literature survey of oxygen species detected at different temperatures on SnO_2 surfaces with infrared analysis (IR), temperature-programmed desorption (TPD), and electron paramagnetic resonance (EPR). Data extracted from [24].

Analysis of the literature indicates that gas sensors are fabricated mainly using either ceramic or thick film technology [18]. These sensors typically have a thickness of gas-sensitive layer of more than 10 μm. However, experiments have shown that sensitivity to ozone in these sensors usually considerably concedes sensitivity to the ozone of the sensors manufactured on the base of thin film technologies, when the thickness of gas-sensitive layer is not more than 300–500 nm [34, 42, 60, 81]. At present, the limited sensitivity of SnO_2- and In_2O_3-based thin film ozone sensors is less than 5–10 ppb. Thin film sensors also have a faster response in comparison with thick film devices, having a thickness exceeding a few micrometers [43, 44, 82]. This is the reason that this review is devoted to ozone sensors with thin gas-sensitive layers. Such sensors can be fabricated using both the thin film and thick film technologies. Studies have shown that after proper optimization of thick film technology this technology allows forming such thin films.

In [16], we began analyzing ozone sensors based on In_2O_3 and SnO_2 and carried out a detailed comparison of their parameters. In the present paper, we continue considering SnO_2 and In_2O_3 as materials for ozone sensor design. In particular, the present review covers the analysis of the fundamentals of ozone sensor operation, including a description of the mechanisms of ozone interaction with metal oxides, the influence of air humidity on sensor response, and the processes that control the kinetics of sensor response to ozone. One should note that the results of the analysis conducted in this review can also be used when considering ozone sensors developed on the basis of other metal oxides.

2.2. In_2O_3- and SnO_2-Based Conductometric Ozone Sensors. As indicated previously, the conductometric ozone sensors analyzed in the present paper are the most used and studied type of devices designed for the control of toxic and inflammable gases [83–89]. In_2O_3- and SnO_2-based

conductometric ozone sensors are usually planar devices. Planar conductometric sensors have a simple structure [18]. They consist of two elements, a sensitive conducting layer and contact electrodes. Contact electrodes are often interdigitated and embedded in the sensitive layer. The sensing layer (in our case In_2O_3 or SnO_2 films) and electrodes can be fabricated by a number of microelectronic protocols as "single-sided" or "double-sided" designs using thin and thick film technologies. The basis of conductometric sensor operation is the change in resistance under the effect of reactions (adsorption, chemical reactions, diffusion, and catalysis) that take place on the surface of the sensing layer [18, 24–31]. Chemical species (ozone, in our case) interact with the sensitive layer and, due to the electron exchange between adsorbed species and the metal oxide, modulate its electrical conductivity. The change in conductivity is correlated to the concentration of the chemical species (ozone in air) and can be measured using DC voltage applied to the device. Sensor response to ozone is, as a rule, calculated as the ratio of the resistances measured in the atmospheres containing and not containing ozone ($S = R_{ozone}/R_{air}$).

For the activation of surface reactions that take place during gas detection, conductometric ozone sensors operate at a high temperature as a rule [18]. For this purpose, gas sensors have incorporated a resistive heater, made usually in the form of a meander, which dissipates the Joule power. Planar sensors are very robust; the temperature homogeneity over the sensing layer is good. It is necessary to note that thick film and thin film technologies are frequently combined to produce planar ozone sensors, especially in laboratory investigations. For example, gas-sensing polycrystalline SnO_2 and In_2O_3 layers may be prepared via thin film technologies (e.g., spray pyrolysis, magnetron sputtering, laser ablation, or chemical vapor deposition), while the heaters are formed with thick film technology [18].

3. General Characterization of In_2O_3- and SnO_2-Based Conductometric Heated Ozone Sensors

It was found that appreciable responses of both SnO_2- and In_2O_3-based ozone sensors arise at $T_{oper} > 100^\circ$C (see Figure 5) [44, 45]. These responses were kept at an acceptable level in a wide temperature range of up to 400–450°C. In most cases, the maximal response to O_3 was observed at T_{oper} = 200–350°C. This temperature range of maximum sensor response is typical for practically all SnO_2- and In_2O_3-based ozone sensors developed, independently from fabrication technology used [33, 34, 41, 51, 55, 58, 90, 91]. It is important that other metal oxides, such as n-ZnO, p-CuO, p-$SrTi_{1-x}Fe_xO_3$, α-Ag_2WO_4, and Fe_2O_3, have maximum response to ozone in the same temperature range [74, 92–94]. For comparison, the maximal response of undoped SnO_2- and In_2O_3-based sensors to reducing gases (CO and H_2) takes place at appreciably higher temperatures—$T_{oper} > 400$–450°C (see Figure 5).

One should note that, for the best In_2O_3 samples (grain size ~5–8 nm), the response to ozone can achieve 10^5–10^6 even for 60 ppb of ozone [51]. Of course, such sensitivity is excessive for real applications. Sensors with an extremely high response usually have a narrow range of detectable ozone concentration and poor stability due to strong sensitivity to the influence of outside factors, such as air humidity, temperature, interference, and poisoning. Experience has shown that response ~10^2–10^3 at 1 ppm O_3 is the sufficient one for market of ozone sensors.

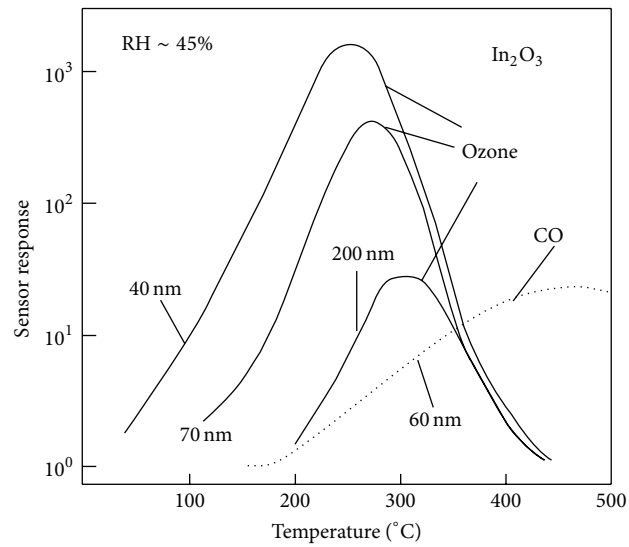

Figure 5: Film thickness influence on temperature dependences of In_2O_3 response to ozone (1 ppm). T_{pyr} = 475°C. Data extracted from [43, 44, 90].

We admit that there are also some papers that report a maximum response to ozone in the range of 100–200°C [33, 35, 42]. However, we cannot explain such a strong distinction. There is an assumption that the changing of the grain crystallographic structure with corresponding changes of facets and point defect concentration could affect this distinction [37, 97, 98]. In particular, our experiments have shown that the temperature of the maximum sensor response (T_{oper}(max)) depends strongly on the grain size, deposition temperature [45], and film thickness [57]. In other words, T_{oper}(max) depends on the parameters that influence the shape of the crystallites (i.e., crystallographic planes participated in gas-sensing reactions). The results of the XRD and TEM measurements confirm this fact [96, 99–103]. In particular, the data presented in Table 4 show that there are many crystallographic planes, which can form facets in crystallites and can therefore participate in gas-sensing effects. Models of several of the most stable SnO_2 and In_2O_3 crystallographic planes are shown in Figure 6. It can be seen that every crystallographic plane is characterized by a specific concentration and configuration of surface atoms (i.e., every plane has its own specific electronic, thermodynamic, adsorption, and catalytic properties) [80, 97, 103–105]. For example, according to the results of the theoretical simulation carried out by Agoston [80], for In_2O_3, (1) the surface stability of stoichiometric In_2O_3 surfaces increases in the order (111) > (011) > (211) > (001); (2) most stable surfaces ((111) and (011)) do not exhibit significant stoichiometric variations, whereas

Table 4: Crystallographic planes, which can participate in gas-sensing effects.

Metal oxide	Planes, which can form facets in crystallites	References
In_2O_3	(010), (100), (111), (110), (00$\bar{1}$), (001), (101), (011), (1$\bar{1}$1), (1$\bar{1}\bar{1}$), (11$\bar{1}$), (211)	[110–112]
SnO_2	(111), (200), (020), ($\bar{1}\bar{1}$2), ($\bar{1}$20), (1$\bar{1}$0), (101), (0$\bar{1}$1), (011), (10$\bar{1}$), (010), (001), (100), (110), (0$\bar{1}$0), (010), (1$\bar{1}$0), (100), (2$\bar{2}$1), (221), (22$\bar{1}$)	[99, 112, 113]

surfaces with polarity, such as (001), can be significantly off-stoichiometric. The largest stoichiometry variations take place for the (001) surfaces, which partially resemble the chemistry of the (211) surfaces and step edges of the (111) surfaces; (3) the chemistry of In_2O_3 surfaces depends on orientation. While most stable surfaces (111) and (011) are characterized by their chemical inertness up to low oxygen chemical potentials close to the material stability limit, the (001) surfaces exhibit various surface phase transitions, which are sensitive to experimental boundary conditions. In other words, gas surrounding (4) hydroxylation of the polar (001) surface is effective in reducing the surface energy to values comparable to or even lower than those of other faces. This is because water adsorption is relatively weak on the more stable (011) and (111) surfaces and locally restricted to a small fraction of the total surface area. Nevertheless, dissociative water absorption is still possible on those surfaces also. The same can be said of the various crystallographic planes of SnO_2 [37, 97]. These results indicate that an explanation of the sensing properties of the oxide nanocrystals cannot be simply provided in terms of the grain size effect [24, 106–109] but must also refer to the specific transducing properties of the nanocrystal surface [37, 51, 97, 98]. However, a large number of crystallographic planes, which can be simultaneously present in the faceting of the crystallites, the strong dependence of crystallite faceting on the crystallite size, and the technological route used for crystallite synthesis or deposition, complicate this task considerably [99, 102, 110–114]. Perhaps only epitaxial films and nanobelts can be used for designing sensors in which only one crystallographic plane will work [97, 104].

A distinctive feature of ozone sensors is the essential difference in response (τ_{res}) and recovery (τ_{rec}) times observed for dry atmosphere (see Figure 7) [43, 56]. Experiments have shown that the response of In_2O_3 and SnO_2 thin films deposited by spray pyrolysis is very fast. Even at $T_{oper} \sim 200^\circ$C, the response time of sensors with optimal thickness ($d < 60$–80 nm) in a dry atmosphere does not exceed 1-2 sec. One should note that, in a wet atmosphere, the response time changes substantially [43, 56, 115]. It was found that the influence of water increases strongly with the decrease in grain size [109], and this influence depends on the operating temperature [56]. In low temperature range, the influence of the water vapors on the kinetics of sensor response intensifies [54].

Recovery is much slower ($\tau_{rec} \gg \tau_{res}$), and τ_{rec} is considerably weaker depending on the humidity of the tested gas. For comparison, during the detection of reducing gases, such as CO and H_2, $\tau_{rec} \approx \tau_{res}$ [116]. According to [117], the indicated behavior ($\tau_{rec} \gg \tau_{res}$) is peculiar for the adsorption/desorption mechanism of gas sensitivity. As is known, in

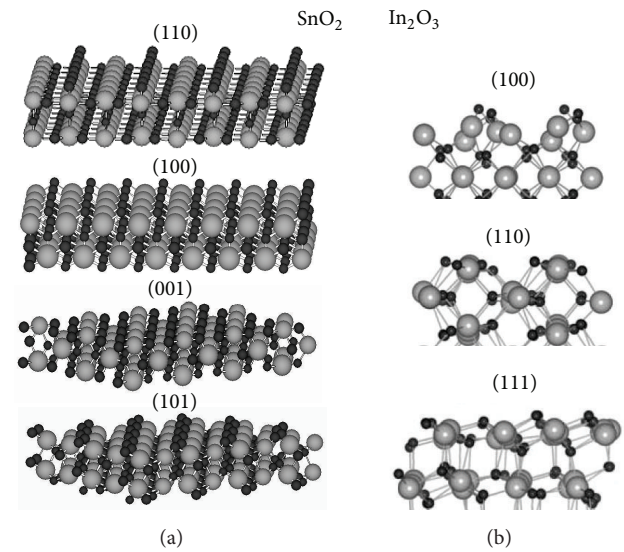

Figure 6: Models of (a) unrelaxed (110), (100), (001), and (101) rutile SnO_2 surfaces and (b) relaxed (100), (110), and (111) bixbyite In_2O_3 surfaces. The large light balls represent tin or indium atoms and the dark small balls oxygen atoms. (a) Reprinted with permission from [95], Copyright IOP. (b) Reprinted with permission from [96]. Copyright 2010 Royal Soc. of Chemistry.

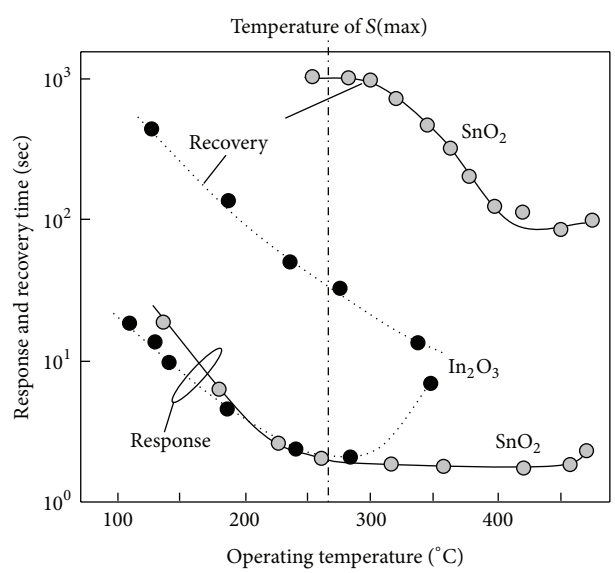

Figure 7: The influence of operating temperatures on the response and recovery times of In_2O_3- and SnO_2-based sensors during ozone detection in dry atmosphere. Tested films were deposited at T_{pyr} = 475–520°C and had thickness $d \sim 30$ nm. Data extracted from Korotcenkov et al. [53, 56].

the case of reducing gas detection, the response is controlled mainly by the catalytic reaction of oxidation. The necessity of both the time desorption increase and the time adsorption decrease of chemisorbed particles is one of the important conditions for achieving the maximum response of solid-state gas sensors, predicted in the frame of the adsorption mechanism of gas sensitivity [117]. The short adsorption time and long desorption time correspond to the condition for higher surface coverage of the adsorbed species of target gas and hence the maximum change in the electrical properties (i.e., resistance) at a given concentration of the target analyte. In full correspondence with this statement, for both In_2O_3 and SnO_2 ozone sensors, we observe the fulfilment of the following correlation:

$$S \sim \left(\frac{\tau_{\text{rec}}}{\tau_{\text{res}}}\right)^m, \tag{4}$$

where m = 1.0–1.5 [43, 45]. The bigger the $\tau_{\text{rec}}/\tau_{\text{res}}$ ratio is, the greater the sensor response is. However, it is necessary to take into account that the increase in film thickness reduces the difference between response and recovery times indicated above. Additionally, for thick films, we have the trend of $\tau_{\text{res}} \rightarrow \tau_{\text{rec}}$ [53]. This means that the processes that control the kinetics of sensor response depend on the film thickness and can be changed.

Regarding the dependence between sensor signal and ozone concentration, we can say that, as a rule, these dependences (see Figure 8) can be described with the power equation [26]:

$$S = \frac{R}{R_0} = KC^X, \tag{5}$$

where X and K are constants; C is the ozone concentration in the air; and R_0 and R are stationary sensor signals in the air without ozone and in the presence of ozone, respectively. Unfortunately, the values of X and K are not constant for various sensors. For example, in the literature on X, one can find that values have varied from 0.2 to 1.5 [50, 55, 123, 124]. Experimental studies and phenomenological modeling have shown that the power exponent X can, in principle, be derived from the mass action laws and rate constants of the respective surface reactions and the relationship between the sensor resistance and the trapped charge density of chemisorbed species [25–27, 125–127]. In practice, however, this derivation is complicated, because the relationship between the resistance and gas concentration depends not only on the surface chemical reaction, but also on the morphology of the sensor, such as a compact (nonporous) thin film or porous thick layer, and on its microstructure (the grain size, the neck area between partially sintered grains, the inhomogeneous distribution of the grain size, the pore size, and other microstructural features) [24, 30, 128–130]. Thus, the present situation with a great range in X values means that, firstly, the metal oxides studied in different laboratories as ozone-sensing materials have a significant difference in structure, and, second, the response of sensors fabricated in different labs can be limited by various processes.

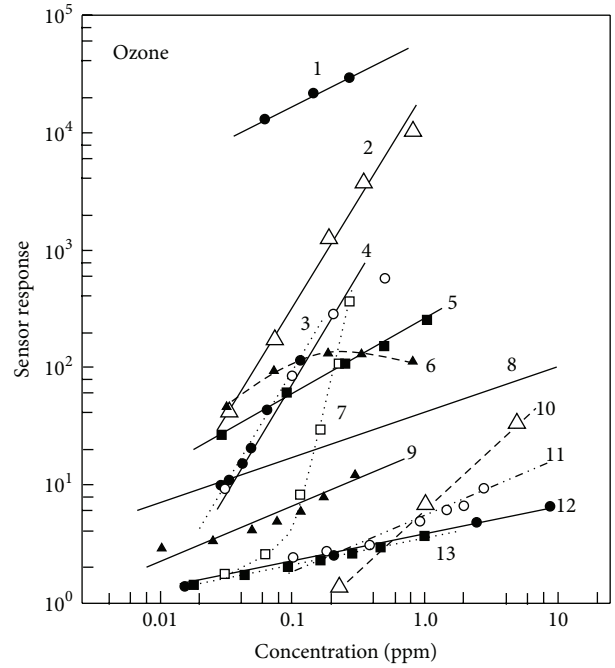

Figure 8: Sensor signal dependences on the O_3 concentration determined for devices designed in different labs: 1: In_2O_3 (sol-gel + drop coating technologies, $t \sim$ 3.5–8 nm, T_{oper} = 300°C) [50]; 2: In_2O_3 (sol-gel + spin coating technologies, T_{oper} = 235°C) [33]; 3: In_2O_3 (laser ablation, $d \sim$ 20–50 nm, T_{oper} = 330°C) [34]; 4: In_2O_3 (sol-gel, $t \sim$ 12 nm, T_{oper} = 235°C) [118]; 5: In_2O_3 (mesoporous, UV illumination, T_{oper} = RT) [119]; 6: In_2O_3 (sol-gel + screen-printing technologies, T_{oper} = 235°C) [33]; 7: SnO_2:Pt (2%) (laser ablation, T_{oper} = 120°C) [35]; 8: In_2O_3:Fe (3%) (CVD, T_{oper} = 370°C) [120]; 9: In_2O_3 (MOCVD, $t \sim$ 7–12 nm, UV illumination, T_{oper} = RT) [121]; 10: In_2O_3 (laser ablation, T_{oper} = 84°C) [35]; 11: In_2O_3 (sol-gel, T_{oper} = 200–300°C) [14]; 12: In_2O_3 (MOCVD, UV illumination, T_{oper} = RT) [15]; 13: ITO (3% Sn) (sol-gel + dip-coating technologies, $d \sim$ 0.1–0.2 μm, T_{oper} = 360°C) [122].

4. Mechanism of Ozone Interaction with Metal Oxide Surface in Heated Ozone Sensors

One should note that, until now, the sensing mechanism of oxidizing gases, such as O_3, has been a matter of debate [53, 54, 58, 123, 131–134]. Due to the acceptor character of the surface state induced by the O_3 chemisorption (these states can trap significant amounts of electrons from the conduction band), ozone ionosorption is accompanied by an increase in negative charge at the surface of an n-type semiconductor and an increase in band-bending ($q\Delta V_S > 0$). For an n-type semiconductor, this results in the creation of a depletion layer at the surface of the metal oxide grains and a decrease in the conductance of intercrystallite barriers, which control the conductivity of polycrystalline materials [$G_0 \sim \exp(qV_S/kT)$]. In this case, the sensor response can be expressed as

$$S = \frac{G}{G_0} \sim \exp\left(\frac{q\Delta V_S}{kT}\right) < 1, \tag{6}$$

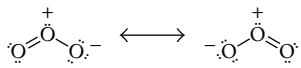

Figure 9: Resonance Lewis structures of the ozone molecule.

where G_0 and G denote the surface conductance before and during oxygen ionosorption, respectively. The mobility of charge carries changes slightly in comparison with concentration [52].

The analysis of possible chemical reactions of In_2O_3 and SnO_2 with ozone [55, 58, 60, 123] allows the proposal of the following reactions, which give the clearly expressed acceptor character of ozone interaction with metal oxide:

$$O_3\,(g) \longrightarrow O_3\,(s) + e^- \longrightarrow O_3{}^-\,(s) \tag{7}$$

$$O_3\,(g) \longrightarrow O_3\,(s) + e^- \longrightarrow O_2\,(g) + O^-\,(s) \tag{8}$$

In this reaction, e^- is a conduction electron in the oxide film, $O^-(s)$ and $O_3{}^-(s)$ are surface oxygen ions, and $O_3(g)$ and $O_2(g)$ are the adsorbing ozone and desorbing oxygen molecules, respectively.

However, by analogy with O_2, which has a larger dissociation energy than O_3 [123, 135] but already adsorbs dissociatively at the surface of SnO_2 at $T > 150$–180°C [86, 136], we believe that, at $T_{oper} > 100$–150°C, reaction (8) (i.e., dissociative O_3 absorption) is preferred [60, 123]. The same statement can be found in [42, 123]. It is known that ozone is a highly unstable molecule that readily donates its extra oxygen atom to free radical species. The geometry of the ozone molecule is such that it has a significant dipole moment, and the central oxygen atom has a lone pair of electrons. In other words, the central atom possesses a positive charge, and one of the side atoms possesses a negative charge (see Figure 9). Therefore, it is quite reasonable to assume that this atom interacts with the metal oxide surface and forms an acceptor, whereas the other two atoms form an oxygen molecule that returns to the gas phase, as shown in reaction (8).

This statement finds confirmation in the results reported in [123, 136, 137], which demonstrate that molecular O_3 was observed at the surface of metal oxides at $T < 300$ K only. At a higher temperature, O_3 was not stable. As is known, ozone has significantly lower dissociation energy than oxygen; dissociation energies for ozone and oxygen are 1.1–1.3 eV and 5.1 eV, respectively [138, 139]. There is only one investigation [140] that has shown the formation of $O_3{}^-$ on the metal oxide surface (CeO_2) interacting with ozone at temperatures below 65°C. Moreover, O_3 adsorption in the form of $O_3{}^-$ should lead to the formation of localized dipoles on the surface [91, 141]. However, additional signals derived from directed dipole layers adsorbed at surface states were not observed in In_2O_3 interacting with O_3, even at 130°C [91, 141]. One can assume that, similar to oxygen, ozone dissociatively adsorbs on the reduced surface cations of Sn (Sn^{2+}) and In (In^{2+}) [78, 142]. As is known [31, 143], the active sites of adsorption on a metal oxide surface are coordinatively unsaturated metal cations and oxygen anions. Metal cations as electron-deficient atoms with vacant orbitals exhibit Lewis acid properties, while oxygen anions act as a base. A schematic diagram illustrating

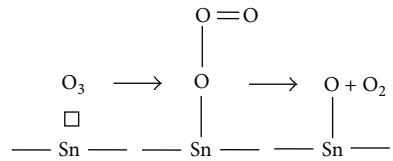

Figure 10: Schematic diagram illustrating process of O_3 dissociative adsorption at the surface of SnO_2 in dry air. Idea from Bulanin et al. [136].

this process for SnO_2 is shown in Figure 10. It is important to note that, in addition to Lewis acidity, metal oxides also possess Brønsted acidity, which is defined as the ability to protonate bases (H^+-transfer) [31]. This type of acidity is the result of the dissociative adsorption of water molecules on the oxide surface for forming protons (H^+) and hydroxyl groups (OH^-). The driving force of these processes is the interaction between a Lewis acid (cation on the metal surface) and its conjugate base (the oxygen atom in a molecule of H_2O). A proton (Lewis acid) formed as a result of this dissociation is captured and tightly binds the surface lattice oxygen atom of the metal oxide (Lewis base), while a hydroxyl group (base) is fixed to the metal cation (acid).

Of course, the process of oxygen incorporation in the metal oxide lattice can also be involved in the reaction of ozone detection. For example, this reaction can be presented using the Kroger-Vink notation as the pathway:

$$O_3 + V_O{}^{\bullet\bullet} + 2e \rightleftharpoons O_O + O_2 \uparrow \tag{9}$$

Equation (9) represents the exchange reaction of oxygen between the gas phase and the metal oxide lattice, in which the predominant defects are oxygen vacancies. As is known, oxygen vacancies are the main point defects in metal oxides. In general, as shown in (9), oxygen adsorption and incorporation into the lattice decrease the free carrier (electron) concentration in n-type metal oxides. However, one should take into account that reaction (9) for SnO_2 is valid for the bulk of the metal oxide only. It was found that oxygen incorporation in the surface vacancies of the SnO_2 lattice is not accompanied by the capture of electrons from the conduction band [105, 144]. This means that, for the indicated electron exchange, the process of oxygen incorporation should be accompanied by bulk diffusion. However, experiments related to the study of metal oxides, such as SnO_2, TiO_2, and $SrTiO_3$, have shown that, in the temperature range below 500°C, the incorporation reaction of the adsorbed oxygen atoms into the lattice (i.e., bulk diffusion) is very slow; therefore, the oxygen exchange reaction is effectively blocked [145–149]. As a result, the oxygen vacancies in the bulk are unable to equilibrate with oxygen from the gas phase. Therefore, for most metal oxide conductometric gas sensors that operate in the temperature range between 100°C and 500°C, chemisorption is the dominant effect that controls the sensing mechanism as a rule. Only at higher temperatures (typically above 500–700°C) does the incorporation into the lattice of metal oxides become the dominant mechanism responsible for the change of their resistance, which takes place due to the bulk oxygen diffusion. DFT calculations of

the SnO_2 (101) surface support this conclusion, suggesting a self-limiting mechanism for the oxygen exchange reaction at temperatures below 400°C [150]. In this temperature range, SnO_2 sensors show the maximum response to ozone.

However, it is important to note that the surface stoichiometry of metal oxides during interaction with a surrounding gas can be changed despite the invariance of the bulk stoichiometry. In particular, Korotcenkov et al. [53, 54] have used this approach based on surface reduction/reoxidation processes to gain an understanding of gas-sensing effects in In_2O_3-based ozone sensors. Korotcenkov et al. [53] believe that, at $T_{oper} > T_{th} \sim 120$–$150°C$, the surface stoichiometry and thus the electronic and surface properties of In_2O_3 grains can be changed under the influence of the surrounding atmosphere. The threshold temperature (T_{th}) corresponds to the temperature below which the oxygen can only be adsorbed on the surface of indium oxide without incorporation into the lattice. These results are in agreement with the data reported by Himmerlich [151]. Himmerlich [151] did not observe oxygen incorporation in the In_2O_3 lattice at room temperature either. Moreover, he has shown that the In_2O_3 band gap in the surface layer can be changed under reduction/reoxidation reactions.

One should note that the maximal sensitivity of SnO_2- and In_2O_3-based sensors to ozone is observed in a temperature range when the surface of metal oxides is free from molecular water ($T > 100°C$) and the concentration of chemisorbed atomic oxygen at the surface of metal oxide is still low [45, 56]. A diagram illustrating the change of the surface species concentration on the SnO_2 surface is shown in Figure 11. Such a situation seems natural to us, because molecular water apparently blocks the sites for dissociative ozone absorption or transforms ozone into another form. For example, earlier in [152], it was reported that SnO_2 surface dehydroxylation is required to obtain an increase in the surface coverage of charged oxygen species adsorbed at the specific surface sites. Bulanin et al. [136] also found that the adsorption of water, in the case of a totally hydrated CeO_2 surface, completely poisoned the sites of molecular O_3 chemisorption. It is also known that the interaction between the oxygen of water and the central oxygen of ozone produces a stable H_2O-O_3 complex [153]. The necessity of a low initial concentration of chemisorbed oxygen is also understandable, because this value determines the possible range of the surface charge change (i.e., the change of surface potential (V_S) during interaction with ozone). As is known, the concentration of chemisorbed oxygen controls the initial band-bending of metal oxides. In addition, the presence of initial chemisorbed oxygen at the surface of metal oxides can initiate reaction (10), which also reduces a sensor response through the consumption of the ozone part involved in surface reactions. Consider the following:

$$O_3\,(g) + O^-\,(s) \longrightarrow 2O_2 \uparrow + e^- \qquad (10)$$

We believe that increased operation temperature also resolves the problem of the surface carbon. Certainly, in real conditions, black carbon [the energetic position of the C1s peak corresponds to the highly ordered pyrolytic graphite phase of carbon] is present in high concentrations at the surface of metal oxides. According to [154, 155], the surface concentration of carbon at room temperature corresponds to 0.5–0.8 of monolayer. Annealing in a vacuum decreases the surface concentration of carbon. However, in the air, the initial concentration of carbon is restored even at room temperature. The correlation established by Brinzari et al. [154] between carbon surface concentration and peak intensities (Sn3d and O1s), corresponding to SnO_2 lattice atoms, has shown that the intensity of the Sn3d peak has a stronger dependence on the surface concentration of carbon species in comparison with O1s (see Figure 12). Such different behavior allows the assumption that the carbon on the SnO_2 surface is bonded predominantly to Sn_{Sn}, which is also the adsorption site for the dissociative adsorption of ozone. This means that carbon is also a poison for O_3 dissociative adsorption. Ozone exposure removes C-related contamination from the metal oxide surface, including SnO_2 and In_2O_3 [155, 156]. Interaction with ozone changes C-related compounds adsorbed onto the metal oxide surface into volatile species, such as CO_2 or CO. However, at RT, this process is comparatively slow. Experiments have shown that even at a high concentration of ozone (up to several vol.%) an equilibrium state can be achieved during several tens of minutes [156, 157]. Thus, operation at higher temperatures either increases the rate of carbon oxidation (i.e., its removal) or increases the rate of CO_2 catalytic decomposition (i.e., the restoration of initial

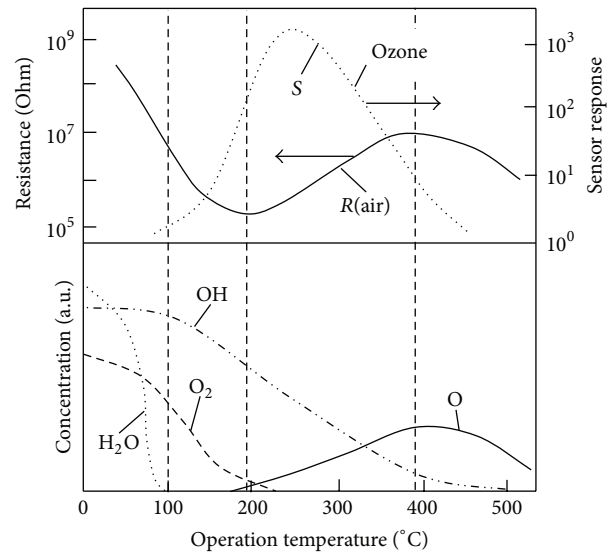

Figure 11: Diagram illustrating processes taking place at the SnO_2 surface during ozone detection: (1) film resistance in air; (2) film resistance in atmosphere containing ozone; (3)–(5) surface concentrations of molecular water, molecular oxygen, and OH-groups, correspondingly; (6) initial surface concentration of chemisorbed oxygen (O^-) determined by oxygen dissociative adsorption; (7) possible addition of chemisorbed oxygen due to dissociative adsorption of ozone. $R(T_{oper})$ measurements were carried out for SnO_2 films deposited at $T_{pyr} = 320°C$. Adapted with permission from [116]. Copyright 2004 Elsevier.

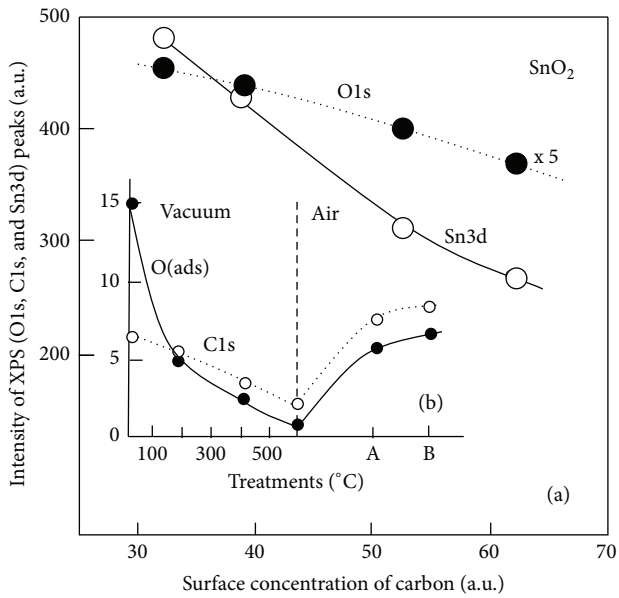

Figure 12: (a) Dependencies of intensities of lattice Sn3d and O1s XPS peaks on surface carbon concentration and (b) influence of various thermal treatments on the intensities of O1s and C1s peaks of SnO_2 X-ray photoelectron spectra ($\varphi = 90^\circ$): A: dry air, $T_{an} = 300^\circ$C, $t = 10$ min; B: humid air, $T_{an} = 300^\circ$C, $t = 10$ min. Data extracted from [154].

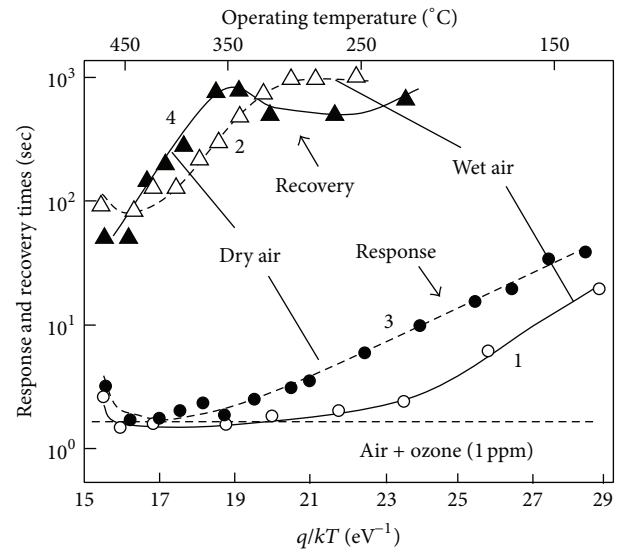

Figure 13: Influence of air humidity on response and recovery times ($\tau_{0.5}$) during ozone detection by SnO_2 thin film sensors (films deposited at $T_{pyr} = 520^\circ$C, $d \sim 30$ nm): 1 and 2: wet atmosphere (~35–40% RH); 3 and 4: dry atmosphere (~1-2% RH). Adapted with permission from [56]. Copyright 2007 Elsevier.

carbon coverage) and thus reduces the influence of these processes on the kinetics of sensor response. Himmerlich et al. [158] have concluded that desorption of carbon species from the In_2O_3 surface activates existing defect sites for interaction with gases, such as ozone. They have also found that this effect has a strong influence on the performance and sensitivity of indium oxide-based gas sensors.

Regarding the recovery process during ozone detection, this process is not as simple as it seems at the first glance. Recovery processes during interaction with ozone are usually considered the reaction of associate oxygen desorption:

$$O^-(s) + O^-(s) \Longrightarrow O_2(g) \uparrow + 2e^- \quad (11)$$

It is clear that this process has the activation nature, because the surface migration of oxygen atoms and electron exchange are required for this reaction. As is known, the ionized chemisorption is limited by the upper band-bending on the material surface [159, 160] (often referred to as the Weisz limitation in the sensor literature). Therefore, the concentration of chemisorbed species cannot exceed 1% from the number of sites possible for adsorption. In other words, the chance of finding chemisorbed oxygen at the nearest surface sites is very low. This means that the rate of this reaction should increase with increasing operating temperature and decreasing band-bending. However, as shown in Figure 13, the temperature dependences on recovery time, especially for SnO_2-based ozone sensors, have at least two sections with specific behavior. At $\tau_{rec} = f(T_{oper})$, the dependences have the activation character only at high temperatures. This means that the recovery processes in various temperature ranges have different natures. We assume that, in addition to the oxygen desorption described by reaction (11), the reactions, such as (12) and (13)–(15), can also take place and control the recovery time. As is known, the surrounding atmosphere contains ~0.5 ppm of H_2 and ~2 ppm of CH_4:

$$O^-(s) + H_2(s) \Longrightarrow H_2O \uparrow + e^- \quad (12)$$

$$2O^-(s) + CH_4(s) \Longrightarrow C + 2H_2O \uparrow + 2e^- \text{ or} \quad (13)$$

$$O^-(s) + CH_4(s) \Longrightarrow CO \uparrow + 2H_2 \uparrow + e^- \quad (14)$$

$$O^-(s) + CH_4(s) \Longrightarrow CH_3 + OH^{\delta-} \quad (15)$$

Data presented in [79, 136, 161, 162] demonstrate that reactions (12)–(15) are possible. In particular, Gatin et al. [162] have studied the adsorption of oxygen and hydrogen at the surface of a film consisting of SnO_2 nanoparticles and have found that molecular hydrogen even at room temperature interacted with adsorbed atomic (chemisorbed) oxygen with formation of water molecules and band-bending change. This means that this reaction does not have a strong limitation in the low temperature range. Bulanin et al. [136] have shown that the atomic oxygen at the surface of TiO_2 appeared due to O_3 decomposition being able to interact with CO with forming CO_2 even at 77 K. Tabata et al. [79] have analyzed the interaction of CH_4 with the SnO_2 surface and found that O^- was consumed through the exposure of CH_4 at 200°C. The effect of water, which is present in the atmosphere, cannot also be excluded [45, 54, 56]. According to reaction (16), the initial state (the particle balance) can be recovered through the O_S^- transformation into hydroxyl groups:

$$O_S^- + H_2O \longrightarrow 2OH^\delta + e^- \quad (16)$$

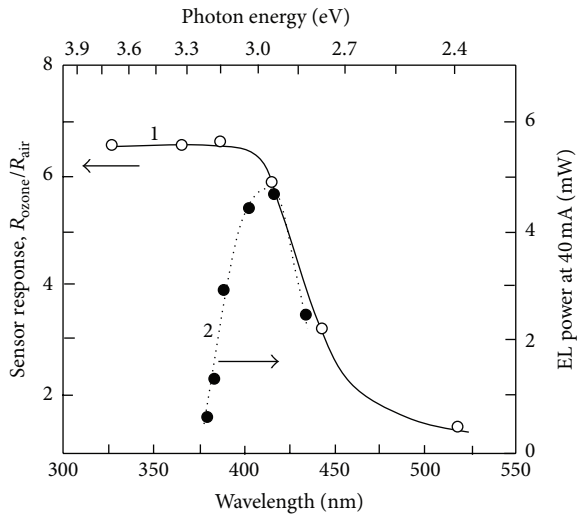

Figure 14: 1: Influence of photon energy on the response of In_2O_3-based RT ozone sensors. 2: spectral characteristics of GaInN QW LED. The layer is irradiated by UV light in vacuum, followed by an oxidation to the original state by means of exposure to O_3. Adapted with permission from [177]. Copyright 2010 Wiley-VCH.

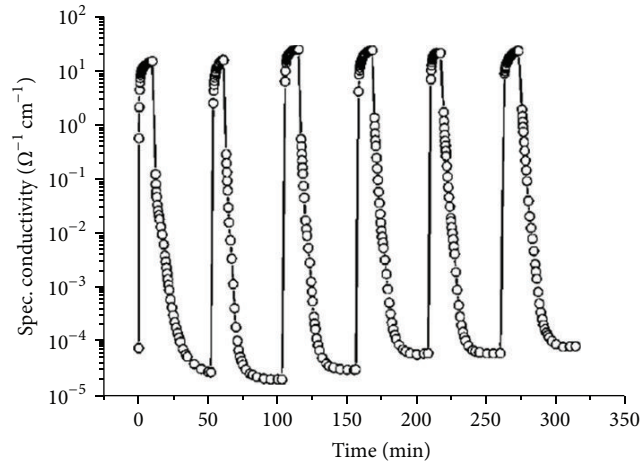

Figure 15: Photoreduction in vacuum and oxidation in oxygen of a 60 nm thick InO_x film deposited by magnetron sputtering at room temperature. Reprinted with permission from [173]. Copyright 2001 American Institute of Physics.

5. Room Temperature Ozone Sensors Operated under the Influence of UV Illumination

At present, there have been attempts to design SnO_2- and In_2O_3-based ozone sensors for operation at room temperature (RT) [141, 163–167]. This type of ozone sensor has recently attracted great interest due to its advantages, such as low energy consumption and the possibilities of integration into plastic packages and portable devices [168]. However, one should note that such sensors usually have very low sensitivity, slow response, poor recovery features, and high sensitivity to air humidity. For example, Epifani et al. [165] reported that the response time of In_2O_3-based ozone sensors at room temperature can exceed 50 min. The involvement of UV illumination in the gas-sensing process considerably improves the operating characteristics of RT ozone sensors [15, 169–172]. Typical parameters of SnO_2- and In_2O_3-based ozone sensors operated at room temperature under influence of UV illumination are listed in Table 5. For comparison, the same table contains information related to the parameters of RT ozone sensors developed based on other metal oxides.

Experiment has shown that indicated improvement of RT ozone sensors takes place due to the strong decrease in the "initial" sensor resistance under the influence of UV illumination. As it is seen in Figure 14, to obtain a maximum value of ozone sensitivity by In_2O_3-based sensor a photon energy higher than ~2.9 eV is required. At photon energy larger than 3.2 eV, the ozone sensitivity remains nearly constant. Thus, the photon energy of UV light from GaN-based LED is acceptable for application in RT ozone sensors, as shown in Figure 14. The similar situation is observed for SnO_2. For significant photoconductivity effect the wavelength of the illumination should not exceed 400 nm [186].

According to general model of photoreduction, UV illumination with $h\nu > E_g$ (3.0–3.7 eV) generates electron-hole pars in metal oxides. The holes generated in the space-charge region are attracted to the surface and can be captured by chemisorbed surface species, such as O_2^-. This process can be described by the following schemes:

$$\{h\nu\} \Longrightarrow e_S^- + h_S^+ \tag{17}$$

$$h_S^+ + O_{2S}^- \Longrightarrow O_{2S} \Longrightarrow O_2 \uparrow \tag{18}$$

In this scheme, $\{h\nu\}$ represents an absorbed photon with energy $h\nu$. The indicated process transforms oxygen species in the neutral form and thus facilitates their desorption (i.e., the photoreduction of the metal oxide). This process, due to an increase of the bulk charge carriers, because the electron of the hole-electron pair remains in the conduction band, and a decrease of the height of the intergrain potential barrier, is accompanied by a strong decrease of metal oxide resistance [171]. The magnitudes of photoreduction are proportional to the UV light intensity. As shown in Figure 15, the reduction at RT in the vacuum is fast. This situation was expected, firstly because the hole injection into the chemisorption states is an exothermic process and, secondly, the oxygen desorption does not require additional reactions.

As mentioned above, the change in the resistance of polycrystalline metal oxide films is ascribed to the change in the barrier height at the intergrain interface. Under these circumstances, the ratio of the resistance measured in the dark and after UV illumination can be approximately expressed in the form

$$\frac{R_{\text{dark}}}{R_{\text{UV}}} \sim \exp\left(\frac{q\Delta\Phi}{kT}\right), \tag{19}$$

where $\Delta\Phi$ is the barrier height change. Taking into account possible changes in the film resistance, particularly data presented in Figure 15, one can find that the reduction of

Table 5: Typical parameters of RT ozone sensors operated using UV photoreduction effect.

Metal oxide	Technology, film parameters	UV source, conditions of photoreduction	Max. S	Conditions of measurements	Response time	Recovery time	References
In_2O_3	Thin film: d~20–110 nm, t~8–25 nm	UV Hg lamp (254 nm), vacuum	~10^5–10^6	RT, ~30–90 ppb	n/a	n/a	[170, 171, 173, 174]
	Thick film (mesoporous): d—n/a, t~30 nm	UV LED, air (100°C)	~130–350	Pretreatment, RT, 0.2–1.2 ppm, dry	Minutes	2.5–5.3 min	[119, 175]
	Thin film: d—n/a, t—n/a	UV LED (375 nm), air (0.1 Pa)	~4	RT, 2.5 ppm	~10 min	n/a	[169]
	Thin film: d~20 nm, t~7 nm	UV LED (375 nm), n/a	~10^5	RT, 10.4 ppm	Minutes	Minutes	[176]
	Thin film: d—n/a, t~7 nm	UV LED (375 nm), air	~5–12	RT, 0.3–1 ppm	Minutes	Minutes	[121, 163, 177]
SnO_2	Thin film: d~450 nm, t—n/a	UV LED (370 nm), air	1.3–1.4	RT, 10 ppm, 60%	Minutes	Tens of minutes	[178]
	Thin film: d~6–9 nm, t—n/a	UV LED (385 nm), air	~1.1	RT, 100 ppb, dry	Tens of minutes	Tens of minutes	[179]
	Thick film: d—n/a, t—n/a	UV light (366 nm), air	26	RT, 2.5 ppm	~50 min	~4-5 min	[180]
Pt/SnO_2	Thick film: d—n/a, t—n/a	UV light (366 nm), air	885	RT, 2.5 ppm	~6 min	~1.5 min	[180]
ZnO	Thin film: d~150–1000 nm, t~5–11 nm	UV Hg lamp (254 nm), vacuum	~10^3–10^8	RT, n/a	Tens of minutes	Minutes	[38, 181]
	Thin film: d—n/a, t~40–100 nm	UV lamp (366 nm), air UV lamp, air (580°C)	~1.2 ~10^3	RT, 2.5 ppm	10 min 1 min	Minutes 5 s (580°C)	[182]
	Thick film: d—n/a, t~40 nm	UV LED (400 nm), air	~2–2.5	RT, 70 ppb, 50%	5–10 min	Minutes	[183]
ZnO-SnO_2	Thick film: d—n/a, t~20/n/a nm	UV light (366 nm), air	39	RT, 2.5 ppm	~2 min	~7 min	[180]
InGaZnO	Thin film: d~65 nm, t—n/a	UV LED (370 nm), air	14	RT, 2 ppm	10 min	>30 min	[184]
TiO_2	Thick film: d—n/a, t~17 nm	UV light (366 nm), air	64	RT, 2.5 ppm	~1 min	~2 min	[180]
	Thick film: d—n/a, t~18 nm	LED (460 nm), air	2	RT, 2.5 ppm	~1.5 min	~1 min	[185]
TiO_2-SnO_2	Thick film: d—n/a, t~17/n/a nm	UV light (366 nm), air	327	RT, 2.5 ppm	~3 min	~15 s	[180]
Pt/(TiO_2-SnO_2) (1 : 4)	Thick film: d—n/a, t~17/n/a nm	UV light (366 nm), air	10^3	RT, 2.5 ppm	~3 min	~1 min	[180]
WO_3	Thick film: d—n/a, t~16–20 nm	LED (460 nm), air	64	RT, 2.5 ppm	~1 min	~1 min	[185]
TiO_2-WO_3	Thick film: d—n/a, t~18/20 nm	LED (460 nm), air	1400	RT, 2.5 ppm	~3 min	~8 min	[185]
Pt/(TiO_2-WO_3) (1 : 4)	Thick film: d—n/a, t~18/20 nm	LED (460 nm), air	2700	RT, 2.5 ppm	15 min	1.5 min	[185]

d: film thickness; t: grain size; S: sensor response (R_{ozone}/R_{air}); conditions of measurements: temperature of operation, gas concentration, and air humidity.

the barrier height in the In_2O_3 films under UV illumination can reach ~0.3–0.4 eV.

Another reason for increasing the RT sensor response under the influence of UV illumination is related to the UV effect on O_3 decomposition. For example, Chen et al. [187] established that the activity of metal oxides toward O_3 decomposition depends greatly on the surface properties of the oxide, the presence of irradiation, and the relative humidity. They have shown that while α-Fe_2O_3 can catalytically decompose O_3 in the dark, the TiO_2 surface is deactivated by O_3 exposure. Under dark conditions, the presence of atmospheric water inhibits O_3 decomposition at room temperature through the competitive adsorption of water molecules and ozone for active surface sites. In the presence of UV radiation under dry conditions, photoenhancement in O_3 decomposition was observed for both α-Fe_2O_3 and TiO_2. The presence of both water and UV radiation leads to more complicated behavior. In particular, it was found that the UV irradiation of TiO_2 leads to an initial increase and a subsequent decrease in ozone uptake coefficients as the RH is increased.

It should also be taken into account that the joint action of UV illumination and ozone stimulates the removal of carbon species [157, 158], which contributes to the activation of the metal oxide surface. As previously described, this process also occurs in the dark but is relatively slow and ineffective as in the presence of UV illumination [156]. In an ozone atmosphere without UV light, efficient surface cleaning requires temperatures of approximately 200°C.

There are also suggestions that the effect of photoreduction/reoxidation on InO_x films is related to the formation and annihilation of oxygen vacancies in the film [188]. According to this mechanism, UV irradiation transfers oxygen from a bound to the gaseous state. In the resulting vacancies the two electrons of the oxygen ion are left in the vacant site and can contribute to the increase in the density of free carriers. The subsequent oxidation in an ozone atmosphere contributes to the incorporation of oxygen into the film, diminishes the density of oxygen vacancies, and therefore leads to a drastic decrease of the available charge carrier concentration. However, for the implementation of this mechanism in polycrystalline materials it is necessary to assume that fast oxygen lattice diffusion occurs even at room temperature, which is unlikely. Therefore, the majority of researchers are inclined to believe that the photoreduction/reoxidation is a surface effect [170].

For UV illumination, different UV Hg lamps [170] or GaN-based LEDs [163] can be used. A typical photoreduction/oxidation cycle for the In_2O_{3-x} films is shown in Figures 15 and 16(a). The processes of photoreduction and oxidation were fully reversible. The description of the mechanism of this interaction can be found in [119, 131, 172].

However, experiments have shown that the sensitivity comparable with that of conventional ozone sensors was achieved only for sensors based on the photoreduction/reoxidation principles, which operated using UV photoreduction in a vacuum or an atmosphere of inert gas. In this case, the photoreduction is carried out in vacuum, but the measurement of sensor response to ozone is conducted

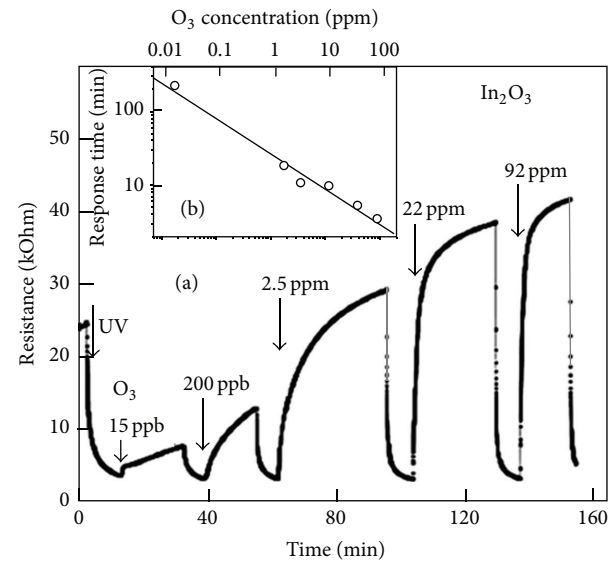

Figure 16: (a) Room temperature resistance change in air of In_2O_3 films deposited by MOCVD ($d \sim 700$–800 nm) at different ozone concentrations. (b) Response times at different O_3-concentrations. For UV illumination, InGaN-LED ($\lambda \sim 375$ nm) was used. Data extracted from [169].

in an atmosphere containing ozone at ordinary pressure. Such sensors based on films with thicknesses of less than 100 nm had extremely high sensitivity to ozone of up to 10^5–10^6 even for the ppb range [15, 170, 171]. It is important to note that the maximum response was observed for the films deposited at low temperatures. Increasing both the deposition temperature (see Figure 17) and the temperature of subsequent annealing significantly reduced this response. Sensor response strongly decreased also with increasing operation temperature (see Figure 18). In all cases, the decrease in sensor response was due to the increase in the conductivity measured in the atmosphere of ozone.

It is clear that the cycle of measurement mentioned above is not convenient for real applications. In addition, the response in the low concentration range is especially slow (see Figure 16). One should also note that when using this method it is difficult to distinguish the influence of ozone and oxygen, because reoxidation also occurs in normal atmosphere (see Figure 15), albeit at a slower rate. This approach also does not take into account the change in conductivity due to net electron-hole generation, which can be several orders of magnitude.

For sensors operated in the usual atmosphere the response is subject to the same regularities that have been established for photoreduction in the vacuum, but the magnitude of the response did not exceed 6–10 for the ppm level of ozone concentration [163, 166, 172, 178]. Only Wagner et al. [119] reported the extremely high sensitivity of In_2O_3-based ozone sensors at RT ($S \sim 350$ at 1.2 ppm O_3). A high sensitivity to ozone was observed in both dry and humid atmospheres. Typical characteristics of these sensors are shown in Figure 19. We cannot explain this result, because there are some papers that report an opposite effect. For

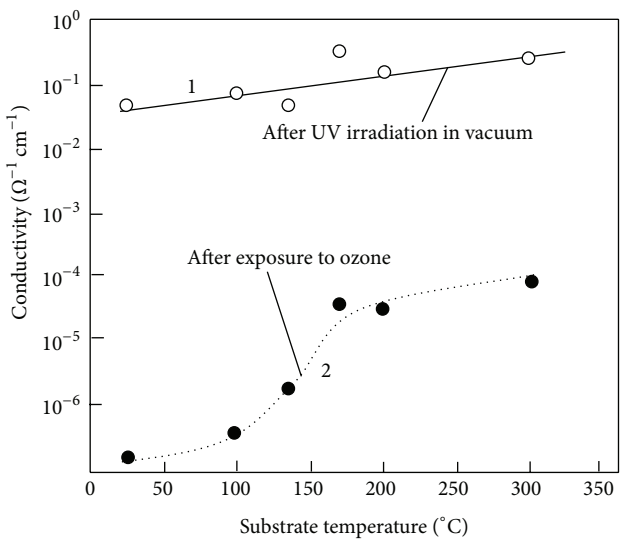

Figure 17: Maximum and minimum conductivities of InO_x films prepared at different substrate temperatures during photoreduction/reoxidation process. Films were deposited by DC-magnetron sputtering. Photoreduction was carried out in vacuum using UV Hg lamp. Adapted with permission from [173]. Copyright 2001 American Institute of Physics.

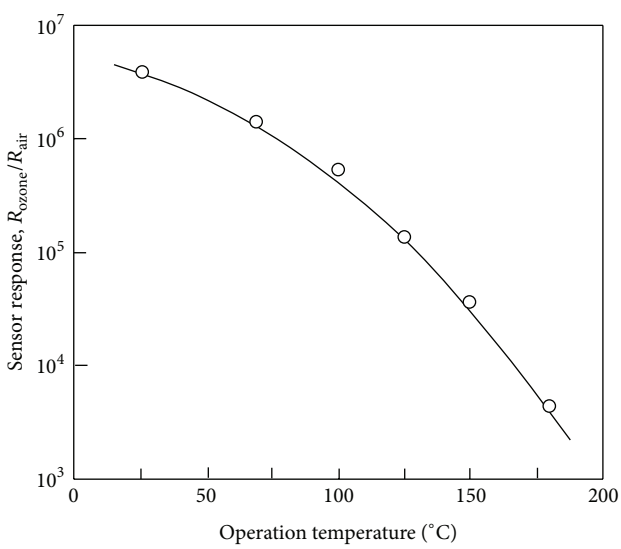

Figure 18: Sensitivity of a 100 nm thick InO_x film versus operation temperature. Films were deposited by DC-magnetron sputtering. Photoreduction was carried out in vacuum using UV Hg lamp. Adapted with permission from [170]. Copyright 2001 Wiley-VCH.

example, Wang et al. [121] have shown that the sensitivity to ozone of UV-assisted In_2O_3 sensors strongly decreased in a humid atmosphere at RT. They observed that the increase of air humidity from 0 to 12% RH was accompanied by a drop of sensor response from $S \sim 100$ to $S \sim 13$. In addition, Munuera et al. [132] have shown in the example of TiO_2 that UV photodesorption from fully hydroxylated surface is a complicated process, because the "photodesorption of water," which can be activated by reaction (20) with forming

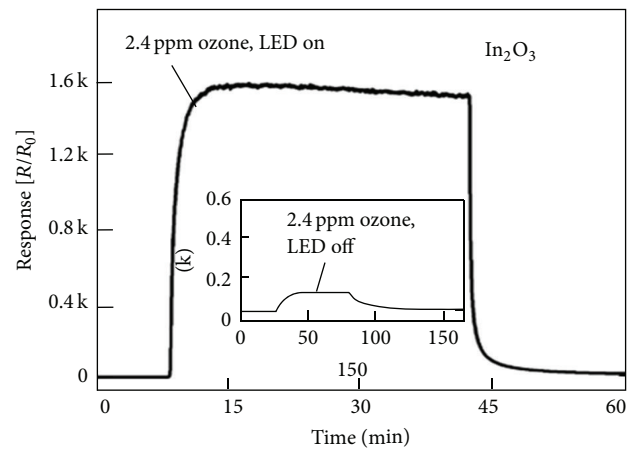

Figure 19: Response of In_2O_3 sensor at room temperature to 2.4 ppm ozone in dry atmosphere with and without illumination by a blue LED (λ = 460 nm) ($d \sim 5\,\mu$m). Data extracted from [119].

$OH^{\bullet}$ radicals, can be accompanied by the photoadsorption of oxygen on these "fully hydrated surfaces." Consider the following:

$$OH^- + \text{h-e} \Longrightarrow OH^{\bullet} + e^- \text{ (free)} \tag{20}$$

Only the thermal removal of water and hydroxyl groups reduced the photoadsorption of oxygen. Munuera et al. [132] assumed that the reduction from Ti^{4+} to Ti^{3+} under irradiation produced a weakening of the bond to the point of desorbing H_2O from the surface. During the diffusion of "excitons" from the "porthole sites" to the trapping sites, desorption of water molecules may occur, with each exciton being responsible for desorption of a certain number of water molecules before oxygen adsorption takes place. This means that the UV photoreduction of the metal oxide surface in humid air is not as effective as in dry air.

Thus, it is possible that the high RT sensitivity of the sensors designed by Wagner et al. [119] in humid air was achieved due to the specific technology used for the In_2O_3 synthesis and, therefore, specific surface properties of gas-sensitive material; mesoporous In_2O_3 used as gas-sensitive material was synthesized by a nanocasting procedure. In addition, the authors did not use the high temperature treatment ($T > 500^\circ$C) to stabilize the properties of the films. Moreover, before each measurement, the samples were subjected to specific pretreatment. The same situation was observed in [182]. Chien et al. [182] have found that a sharp increase in the sensitivity of RT ZnO-based sensors to ozone took place only in that case if the photoreduction was carried out at temperatures above 500°C.

As for the results presented in [176] (see Table 5), there is also some uncertainty about the conditions of the experiment, because the same authors in later articles [121, 163, 177] for the same films provided data on sensitivity to ozone, which at 4 orders of magnitude were lower than data reported in [176]. Apparently, these differences are related to differences in the measurement methodologies used in these articles. In [176], the UV photoreduction was conducted

under synthetic air without ozone, but the measurement of sensor response to ozone was performed at off UV light. In this case we have a situation close to that which was observed during UV photoreduction in vacuum, when it was not possible to separate the contributions of ozone and oxygen presented in the atmosphere in the change of film conductivity, while in [121, 163, 177] UV light was switched on during the whole measurement cycle.

Unfortunately, we have a very limited amount of research in the field of UV assistance RT ozone sensors and very limited information about In_2O_3 and especially SnO_2 films used for the fabrication of these sensors. Therefore, we do not have the opportunity to conduct a detailed consideration of these devices. We can only say that the main requirements of metal oxides aimed toward application in RT ozone sensors [15, 171, 173] coincide with the requirements that have been established for conventional sensors. The response to ozone increased with decreasing grain size [163, 176] and film thickness [174]. For example, Wang et al. [176] reported that an increase in grain size from 7 to 10 nm was accompanied by the decrease in the sensor response from 10^5 to 10.

6. Water Influence on Operating Characteristics of Heated Ozone Sensors

It is necessary to say that water seems to play an important role in the reactions of ozone detection. As is known, metal oxide surfaces can be characterized by their ability to form strong chemical and hydrogen bonds with water molecules [24]. Korotcenkov et al. [53, 54, 56] have shown that water influenced the magnitude of sensor response to ozone, response and recovery times, and the activation energies of processes that control the kinetics of gas-sensing effects. This means that the presence of humidity in the surrounding atmosphere adds complexity to the sensing process, and possible surface reactions should be more complicated, because water can interact with both lattice atoms of metal oxides and adsorbed species, including oxygen and ozone [53, 56, 116, 166]. For example, Căldăraru et al. [189] concluded that the presence of hydroxyl groups at the surface of this oxide limited the oxygen adsorption at temperatures of 320–340°C even under exposure to pure oxygen. In addition, processes such as water dissociation, the protonation of surface groups, and ion surface complexation should be taken into account. A schematic illustration of the behavior of water at the surface of SnO_2 is shown in Figure 20.

However, admittedly, the role of water is not completely understood yet. For example, we are not able to suggest an experimentally confirmed mechanism, which could explain the growth of response in humid air observed for both In_2O_3-[33] and SnO_2-based ozone sensors [56] operated in the temperature range of 200–400°C. It is important to note that, for RT In_2O_3 ozone sensors operated under the influence of UV illumination, the response to ozone decreases with air humidity increases [121]. For comparison, the response of the In_2O_3 and SnO_2 sensors to reducing gases also decreases in humid air as a rule [33, 190]. We believe that only the mentioned effects are connected to the specific role of water both in the reactions of ozone detection and in the mechanism of ozone dissociation at the hydroxylated surface of SnO_2. For example, hydroxyl groups are known to catalyze ozone decomposition [55]. It is also known that the reaction of hydroxylation has a clear donor-like character [191–193] and causes an increase in conductivity and a decrease of band-bending. According to general conceptions [191–193], the water molecules interact dissociatively with defect-free tin oxide by forming a terminal OH-group situated at the Sn_{5c} Lewis acid site, while the proton forms the bridging OH-group with the twofold coordinated O atoms on the next ridge. One of the possible reactions that can explain the above-mentioned behavior of conductivity is presented below:

$$\begin{aligned}&\left(Sn_{Sn}{}^{\delta+}\text{-}OH^{\delta-}\right) + O_3 + \left(O_O\text{-}H^+\right) + 2e^- \\ &\Longrightarrow \left(Sn_{Sn}\text{-}O^-\right) + O_O + O_2 \uparrow + H_2O \uparrow\end{aligned} \tag{21}$$

Here, water desorption results from the ozone-OH interaction. We assume that ozone can form intermediates, such as HO_2 or HO_3 [194–196], during the interaction with the hydrated surface. In this reaction, we did not take into account molecular oxygen and water, because, as shown in Figure 20, at $T > 200°C$, OH-groups and chemisorbed oxygen were dominant at the surface of the metal oxides [56, 116, 197, 198]. Molecular water desorbs from the surface of SnO_2 at $T \sim 100°C$, while molecular oxygen desorbs at $T > 180$–$200°C$. As shown in the right part of (21), the state of the SnO_2 surface after interaction with ozone is the same as the state of the surface after reaction with ozone in a dry atmosphere in this case. This means that hydroxyl groups participate in the reaction of ozone detection; therefore, dissociative water adsorption/desorption can control the kinetics of sensor response to ozone in humid air (read the next section).

When the operation temperature exceeds 350°C, the influence of water vapors on the operating characteristics of ozone sensors is being considerably decreased. As shown in Figure 21, at $T_{oper} > 350°C$, the influence of RH becomes insignificant. In principle, this effect is expected, because it was observed many times for the SnO_2 and In_2O_3 sensors during reducing gas detection. Moreover, this observation is consistent with the results of the temperature-programmed desorption (TPD) and Fourier transform infrared (FTIR) spectroscopic studies of OH-desorption from the SnO_2 surface [197, 199]. These reports show that hydroxyl groups start to desorb at $T > 200$–$250°C$ and are virtually absent at $T > 400°C$. Thus, if there are no limitations in consumable power and we do not have strict requirements of selectivity (in the high temperature range, sensors are sensitive to reducing gases), $T_{oper} \sim 350$–$400°C$ would be optimal for ozone sensor operation in an environment with variable humidity. Certainly, sensitivity in this temperature range decreases, but this reduction is not critical for ozone detection.

7. Processes That Control the Kinetics of Response of Metal Oxide Ozone Sensors

7.1. Heated Ozone Sensors. The previous sections describe the mechanism of ozone interaction with the metal oxide surface

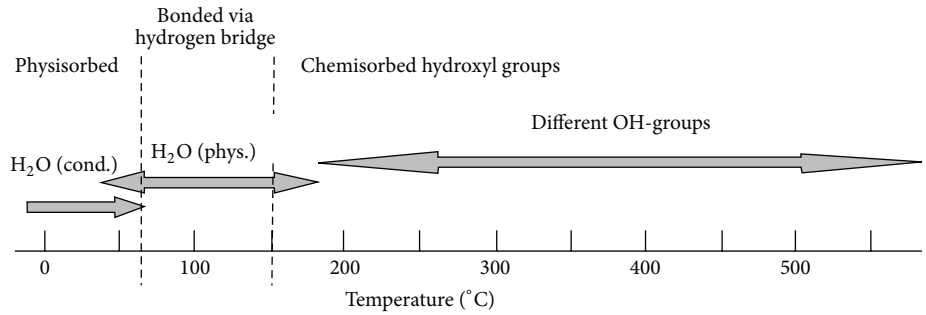

Figure 20: Literature survey of water-related species formed at different temperatures on SnO_2 surfaces. Data extracted from [24].

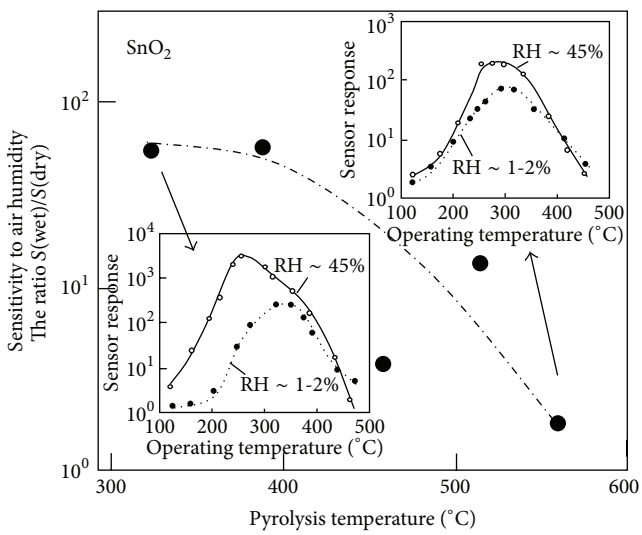

Figure 21: Influence of deposition temperature on the sensitivity to air humidity of SnO_2 sensor response to ozone (~1 ppm). Sensitivity to air humidity was calculated as a ratio of responses measured in dry (1-2% RH) and wet (~45% RH) atmospheres at T_{oper} corresponding to maximum response in humid atmosphere (d ~ 30–50 nm). Adapted with permission from [56]. Copyright 2007 Elsevier.

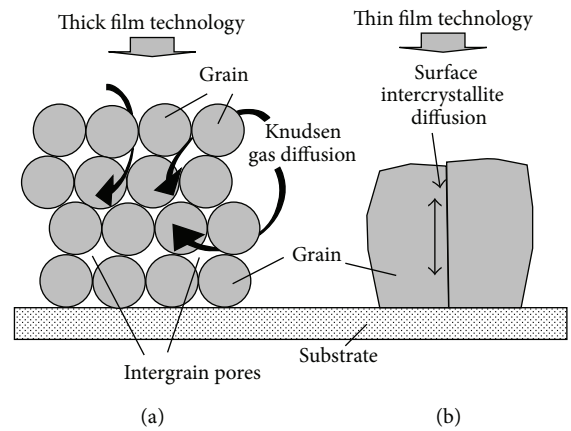

Figure 22: Diagram illustrating difference in structures of the films prepared using "thick" and "thin" film technologies. Reprinted with permission from [57]. Copyright 2009 Elsevier.

but do not answer the question of how this interaction affects the properties of the metal oxide gas-sensing matrix and what processes control the kinetics of these changes. It is clear that the change in conductivity of metal oxides ($\Delta G \sim \Delta n_b$, where n_b is the concentration of free charge carriers in the metal oxide) induced by their interaction with ozone can be controlled by surface and bulk processes [54].

As shown in [57], In_2O_3 and SnO_2 films deposited using thin film technologies are compact, and in spite of a considerably smaller thickness they do not have the porosity found in sensors fabricated by thick or ceramic technologies [86]. Experiments have shown that films deposited using sputtering technologies had an especially dense structure [86, 200]. This means that these films are less gas-permeable in comparison with films prepared using thick film technologies. Typical cross sections of such films are shown in Figure 22. These SEM images show a clear interface between crystallites. This fact points to the absence of necks between grains, whose overlap is usually used to explain the high sensitivity of ceramics-based gas sensors. This means that films deposited by thin film technology have larger contact areas between crystallites. In addition, due to the columnar structure, in which grains can grow through the full film thickness (see Figure 23), the area of the indicated contacts is considerably increased with the film growth. For the thick film sensors the grain size and the area of intergrain contacts do not depend on the film thickness. Taking into account such a situation, Korotcenkov et al. [54] concluded that intercrystallite (surface) diffusion should be involved in the explanation of the gas-sensing characteristics of thin film gas sensors in addition to commonly used surface and bulk processes.

According to Korotcenkov et al. [54], four processes control the magnitude and kinetics of response to ozone (see Figure 24). They are as follows: (1) adsorption/desorption processes and catalytic reactions at the metal oxide surface ($\Delta n_b \sim \Delta N_S \sim V_S$, where n_b is the concentration of free charge electrons in the bulk of grains, N_S is the total concentration of chemisorbed chemical species, and V_S is the rate of surface chemical reactions; and $\Delta G \sim \Delta\phi_S \sim \Delta Q_S \sim \Delta N_S$, where ϕ_S is the height of the intergrain potential barrier and Q_S is the charge on the interface surface states); (2) chemical reactions with lattice (O_L) oxygen participation (reduction/reoxidation) ($\Delta n_b \sim \triangle(\mathrm{Me/O})_b \sim \Delta(\mathrm{Me/O})_s$,

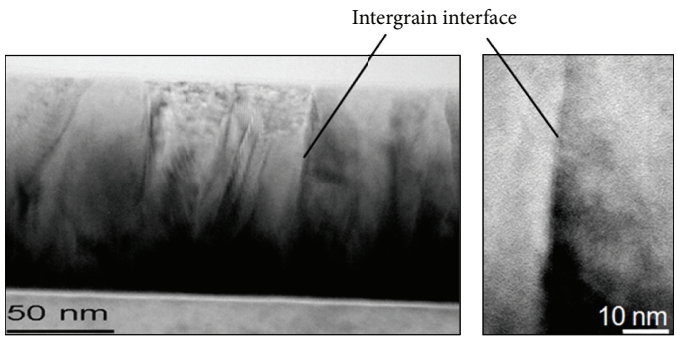

Figure 23: SEM images of the SnO_2 films deposited at $T_{pyr} = 520^{\circ}C$ ($d \sim 120$ nm). Reprinted with permission from [57]. Copyright 2009 Elsevier.

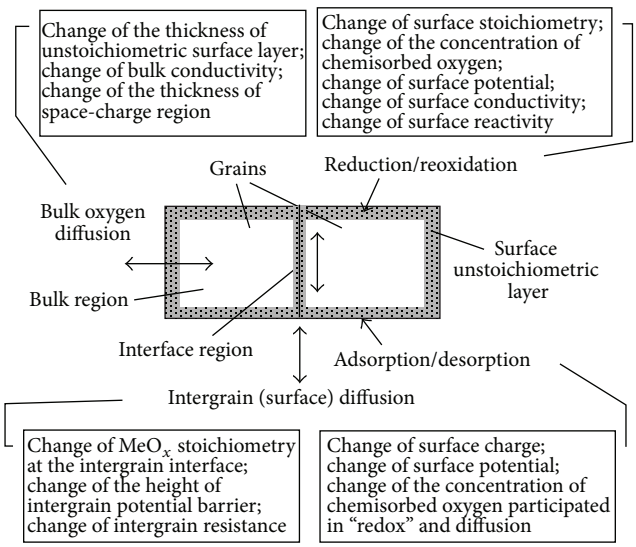

Figure 24: Diagram illustrating surface and bulk processes taking place in metal oxide matrix during ozone detection and their consequences for polycrystalline material properties. Reprinted with permission from [54]. Copyright 2007 Elsevier.

where $(Me/O)_b$ and $(Me/O)_s$ are the bulk and surface stoichiometry of metal oxides, correspondingly); (3) surface and intercrystallite oxygen diffusion, influencing the ϕ_S and $(Me/O)_s$; (4) the bulk diffusion of oxygen (diffusion of oxygen vacancies), which influences the concentrations of ionized centers and the mobility of charge carriers through the change of the concentration of point defects (N_p) in metal oxides ($(\Delta n_b, \Delta\mu_b) \sim \triangle N_p \sim \triangle(Me/O)_b$).

If all the four processes listed above participate in the gas-sensing to a greater or lesser extent, then the transient characteristics of sensor response should be represented as the superposition of the four components related to these processes [54]; that is,

$$\Delta G(t) = K_d(t)\{\Delta G_1(t) + \Delta G_2(t) + \Delta G_3(t) + \Delta G_4(t)\}, \quad (22)$$

where $G_1(t)$ is the change of conductivity connected to the adsorption/desorption processes on the surface of the metal oxide, $G_2(t)$ is the change of conductivity conditioned by the processes of reduction/reoxidation, $G_3(t)$ is the change of conductivity controlled by the intercrystallite (grain) diffusion of oxygen, and $G_4(t)$ is the change of conductivity connected to bulk oxygen diffusion. Taking into account the general character of the discussion, to obtain a full picture, we have introduced in (22) an additional component, $K_d(t)$, which characterizes the rate of delivery of both analyte gas and oxygen to the place where indicated reactions occur. The last process, as is well known, is controlled by the diffusion of analyte gas and oxygen from the surface region of the gas-sensing material into its internal region.

From (22), one can see that two extreme scenarios could occur in ozone sensors, depending on the correlation between the rate of gas diffusion and the rates of processes taking place on the surface and in the bulk of the metal oxide grains. In the first case, the kinetics of sensor response is controlled by the gas diffusion inside the metal oxide matrix:

$$\Delta G(t) = K_d(t)\{\Delta G\}. \quad (23)$$

Such an approach for analyzing the gas-sensing properties of solid-state sensors was developed in [142, 201–210].

It is referred to as a diffusion-reaction model. According to this model, the gas molecules diffuse inside the sensing layer, while they are consumed at a certain rate during diffusion by the surface reaction. This means that the gas-sensing process is considered a phenomenon in which the diffusion and reaction are coupled. Because of this coupling, the response behavior is strongly influenced by the catalytic and microporous properties (gas penetrability) of the sensor material used. As a rule, the diffusion-reaction model describes good kinetics of response of sensors fabricated by ceramics or thick film technology and uses a gas-sensing layer with thickness in the micrometer range.

In the second case, the kinetics of sensor response has been controlled by the processes taking place either on the surface or in the bulk of the grains [54]:

$$\Delta G(t) = \{\Delta G_1(t) + \Delta G_2(t) + \Delta G_3(t) + \Delta G_4(t)\}. \quad (24)$$

The last statement means that the process of gas diffusion into the metal oxide matrix is fast and does not limit the rate of the film conductivity change during the replacement of the gas surroundings. Such an approach to the analysis of gas-sensing effects was considered in [116, 117, 211–213]. As a rule, such an approach has been used for the description of the gas-sensing characteristics of thin film sensors.

It is significant that, during the measurement of the sensor response rate through the estimation of response and recovery times at the level of 0.5 and even 0.9 from the steady-state value of film conductivity, the time constants of response and recovery could not be controlled by the slowest process under certain conditions. They could be controlled by the most influential process (i.e., the one providing the maximal contribution to the conductivity change of the gas-sensing material).

No doubt, the suggested approach to the consideration of gas response kinetics is simplified enough. While making such a consideration, we did not take into account that the analyzed processes are multistage ones [24, 214–216] and, as a rule, comprise electron exchange between adsorbed species and the bulk of the metal oxide. It is known that the adsorption of chemical species without electron exchange (physisorption) cannot be responsible for the change in conductivity of the metal oxide [24, 83]. This means that, under certain conditions, the time of sensor response and recovery during the process of gas detection could be limited by the rate of electron exchange. However, research on SnO_2- and In_2O_3-based CO and H_2 sensors conducted in [53, 116, 211] has shown that, at $T_{oper} > 100^\circ C$, the electron transfer of delocalized conduction band electrons to localized surface states took place quite quickly, and this process was not a factor that limited the rate of sensor response.

The experiment and simulation have shown that surface chemical reactions (reduction/reoxidation) may also take place via a precursor state, the occupancy of which is controlled by adsorption/desorption (a/d) processes [117, 214–216]. In this case, the change of conductivity $\Delta G_3(t)$ could be presented as follows [116]:

$$\Delta G_3(t) = K_{a/d}(t)\{\Delta G_c(t)\}. \quad (25)$$

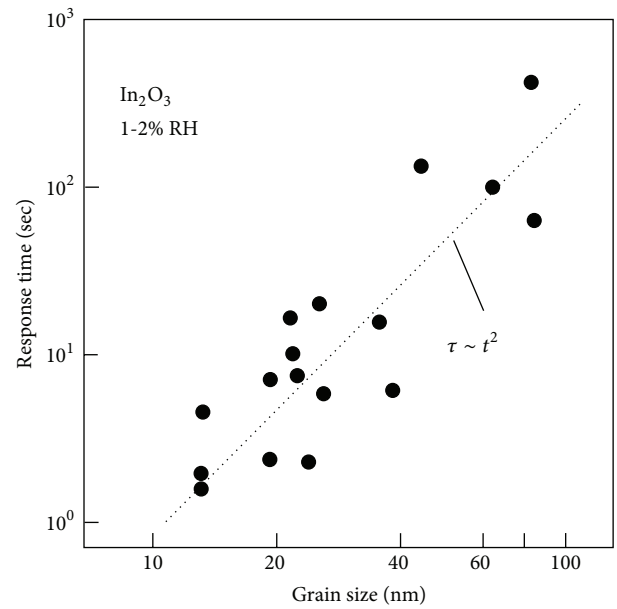

Figure 25: Dependencies of response time during ozone detection ($T_{oper} \sim 270^\circ C$) on the grain size of In_2O_3 films deposited from 0.2 M $InCl_3$-water solution. Reprinted with permission from [43]. Copyright 2004 Elsevier.

This means that the adsorption/desorption (a/d) processes could exactly determine the kinetics of those reactions, as the slowest in this sequence of events. Such a conclusion was made in [116, 117, 211, 212] while analyzing the gas sensitivity of SnO_2-based solid-state sensors to reducing gases. It was established that the kinetics of sensor responses to CO and H_2 was controlled by the processes of oxygen and water adsorption/desorption.

It is significant that if the shape of transient curves $G(t)$ depends on the mechanism of the surface and bulk processes' influence on the metal oxide conductivity [24, 212], the absolute value of the time constants, used for the description of observed changes in metal oxide conductivity, and activation energies, determined from the temperature dependences of response and recovery times, are specific parameters for those surface and bulk processes. As is known [28, 117, 146, 201, 202, 212], processes that control the kinetics of sensor response are activation ones, which have some activation energy specific for each process.

A detailed study of the kinetics of solid-state sensor response to ozone was conducted by Korotcenkov's group for In_2O_3-based devices. The results of this research were reported in [54, 56, 116]. It was found that, in a dry atmosphere (1-2% RH), the response time showed a clear dependence on film thickness (Figure 5) and grain size (see Figure 25), which can be described by the equation $\tau_{res} \sim (d, t)^m$ with index m close to 2 [43]. As is known, such dependence is specific for the diffusion process.

Taking into account the features of the structural properties of thin films [43, 45, 47, 98–102, 109, 114], Korotcenkov et al. [54] have assumed that the above-mentioned diffusion process is intergrain (surface) oxygen diffusion.

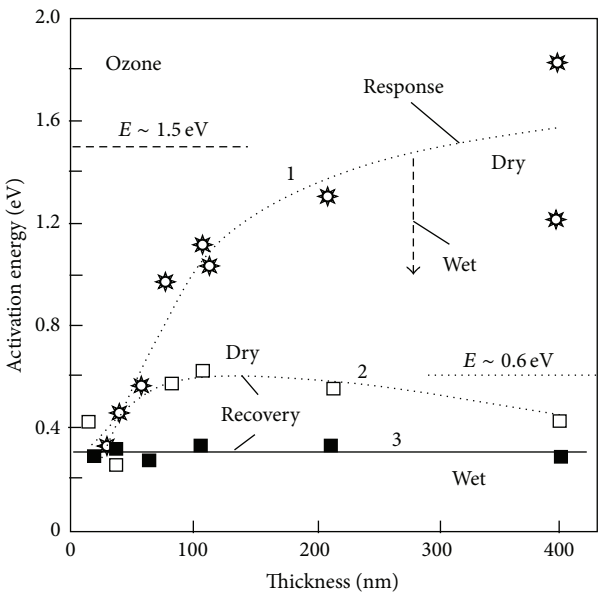

Figure 26: Influence of the film thickness on the activation energies of transient characteristics during ozone detection: (1) response; (2 and 3) recovery; (1 and 2) dry atmospheres (RH ~ 1–3%); (3) wet atmosphere (RH ~ 45–60%); T_{pyr} = 475°C. Reprinted with permission from [54]. Copyright 2007 Elsevier.

Korotcenkov et al. [54] believe that the driving force of this diffusion process (gradient in oxygen chemical potential) may occur due to the change in oxygen concentration $(O/In)_S$ in the surface nonstoichiometric layer. This conclusion was based on the following facts: (1) the In_2O_3 and SnO_2 surfaces are nonstoichiometric, with compositions sensitive to chemical environment changes; (2) only oxygen participates in the reaction of O_3 detection in a dry atmosphere; and (3) $\tau = f(E/kT)$ dependencies determined for In_2O_3-based sensors with thicknesses exceeding 100 nm during the response to ozone in a dry atmosphere at operating temperatures higher than 200–250°C have activation energy equal to 1.2–1.8 eV (see Figures 26 and 27(a)) [54]. Analysis of the literature data confirms that such activation energies correspond to the activation energy of oxygen diffusion in polycrystalline metal oxides, which is controlled by surface or intergrain diffusion and does not exceed 1.5–1.8 eV [217]. For comparison, for bulk oxygen diffusion in metal oxides, including In_2O_3, one can find activation energies in the range from 2.6 to 5.0 eV [200, 218]. As is known, surface diffusion is much faster (~10^5) than bulk oxygen diffusion.

At the same time, the recovery time depends weakly on the film thickness (see Figure 25) and the grain size even at relatively low air humidity (1-2% RH). In addition, in a wet atmosphere, the influence of In_2O_3 grain size on the time constants of gas response to ozone dropped sharply, and the activation energies of $\tau = f(E/kT)$ dependencies were changed (Figure 27(a)). Such behavior of the time constants indicates that the kinetics of sensor response in a wet atmosphere and the kinetics of recovery processes are controlled by several processes, most of which are related to the surface reactions. Analysis of the transient curves of conductivity response to ozone carried out in [53, 54] has shown that the kinetics of recovery processes had two characteristic activation energies (E_{act}) for $\tau = f(E/kT)$ dependencies [54]: (1) 0.25–0.3 eV and (2) 0.5–0.6 eV. The E_{act} ~ 0.5–0.6 eV is peculiar to transient processes of the conductivity response of "porous" films. As a rule, these processes were dominant at T_{oper} > 100°C when a dry atmosphere was used. Processes with the activation energy 0.25–0.3 eV were generally observed during ozone detection in a wet atmosphere. Taking into account that processes with E_{act} ~ 0.3 eV were dominant in ozone detection in a wet atmosphere and processes with the activation energy of ~0.6 eV were dominant in a dry atmosphere, it was assumed that the first one is related to water participation, and the second is associated with oxygen participation in these reactions [54]. This is a real assumption, since only oxygen and water participate in reactions of ozone detection, and only dissociative oxygen adsorption/desorption in a dry atmosphere should control the kinetics of equilibrium achievement between the stoichiometry of the surface layer and the surrounding atmosphere during the recovery process of ozone detection. Regarding the processes with activation energies between 0.25–0.3 and 0.6 eV, which are often observed in experiments, one can say that their appearance is quite ordinary. In a real reaction of ozone detection, both H_2O and oxygen participate simultaneously; therefore, in many cases the reaction of ozone detection can run through two different but interrelated paths. Temperature programmed desorption (TPD) measurements [219] have shown that both chemisorbed oxygen and water were rather strongly bound to the In_2O_3 surface. According to Yamaura et al. [219], after exposure to O_2, significant oxygen desorption from the In_2O_3 surface begins only at T > 500°C. In similar experiments, H_2O began desorbing from the In_2O_3 surface at T ~ 210–230°C, reaching the maximum at T = 400°C. However, even at T ~ 600°C, a sufficient quantity of H_2O, perhaps in the form of OH-groups, remains on the In_2O_3 surface. Thus, the surface species (O_2 and H_2O) in chemisorbed forms (O^- and OH) can exert an influence on the gas-sensing characteristics of In_2O_3 gas sensors over the whole analyzed temperature range.

As shown in Figures 26 and 27(b), in ultrathin films (d < 50 nm) with a small grain size, processes with activation energies of 0.25–0.3 eV are already dominant at RH ~ 1–3%. This observation is important and indicates that, with a grain size decrease into the nanometer range (t < 10 nm), the change of energetic parameters of adsorption/desorption processes at the In_2O_3 surface or the increase of the water role in surface reactions occurs. The change of grain shape is confirmation of the first mechanism. As established in [102], at a thickness of less than 40–60 nm, the In_2O_3 grains lose crystallographic faceting and obtain the shape of spherulite. The increase of water influence both on the gas sensitivity of In_2O_3 films with a small grain size [53] and on NO_x conversion by an In_2O_3-Al_2O_3 catalyst with the smallest In_2O_3 particles [220] is confirmation of the second mechanism.

It should be noted that the diffusion nature of the kinetics of sensor response in a dry atmosphere and the surface

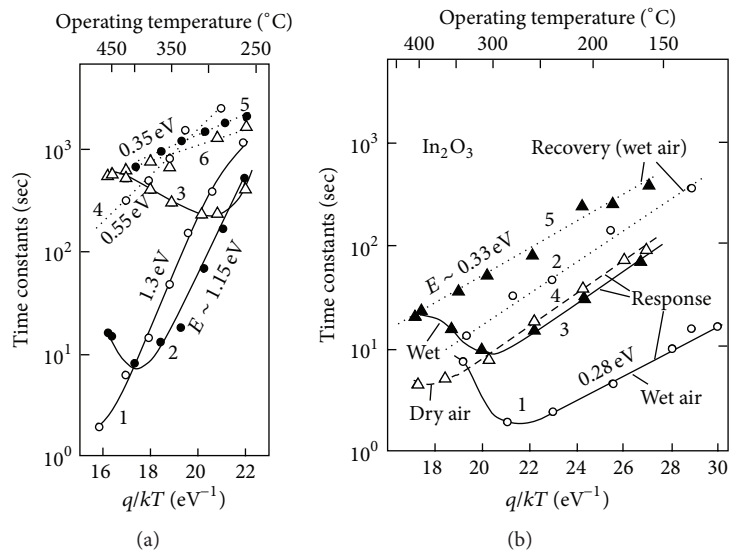

Figure 27: (a) Influence the air humidity on temperature dependencies of (1–3) response and (4–6) recovery times during ozone detection by In_2O_3-based sensors (T_{pyr} = 475°C; d ~ 200 nm; 1.0 M $InCl_3$-solution): 1, 4: ~0.5% RH; 2, 5: ~25–30 RH; (3, 6): ~60% RH; (b) temperature dependencies of the time constants during ozone detection by In_2O_3 ultrathin films in wet (35–40% RH) and dry (1-2% RH) atmospheres (T_{pyr} = 475°C): 1, 2: 0.05 M $InCl_3$-solution, d ~ 20–40 nm; 3, 4, and 5: 1.0 M $InCl_3$-solution, d ~ 40 nm. Adapted with permission from [54]. Copyright 2007 Elsevier.

nature of the reactions responsible for kinetics of both the recovery process and sensor response in a humid atmosphere are not contradictory. Korotcenkov et al. [54] believe that diffusion also participates in processes occurring in a humid atmosphere. However, in this case diffusion is controlled by surface reactions. This means that the concentration of oxygen capable of diffusing and affecting the conductivity of metal oxides via influence on the intercrystallite potential barrier is controlled by the rate of surface reactions [221], particularly in a humid atmosphere, by dissociative water adsorption/desorption processes. These processes control the time of equilibrium establishment between the surface stoichiometry of In_2O_3 and the surrounding gas. The above-mentioned statement that the surface stoichiometry of In_2O_3 can control the surface diffusion processes is very important. Such a conception gives us an understanding of the nature of other effects observed during the In_2O_3 sensor response kinetics study. For example, this conception explains the absence of transient processes controlled by the bulk oxygen diffusion in In_2O_3 even for the transient sensor response measured at T_{oper} > 350°C, when diffusion processes should occur. No doubt, further research is required for understanding in detail the role of diffusion and water in reactions of ozone detection. The question regarding oxygen vacancy participation in the reactions of ozone detection also requires an answer. Namely, is there a change in the concentration of surface oxygen vacancies during ozone chemisorption?

One should note that the approach used for explaining the kinetics of the In_2O_3 ozone sensor response can be applied to SnO_2 ozone sensors as well. In particular, Korotcenkov and Cho [57] have shown that diffusion in the gas phase, including Knudsen diffusion [222] (the approach used for "thick film" and ceramic gas sensors [81, 206, 223]), could not limit the kinetics of response of SnO_2 thin film gas sensors. For films with a thickness of 40–70 nm, it is difficult to imagine the existence of a structure in which the sensitivity is limited by gas diffusion along the pores. Korotcenkov et al. [56] believe that, similarly to In_2O_3, the kinetics of SnO_2 based gas sensors is controlled by intergrain (surface) diffusion and surface reactions, such as the adsorption/desorption of water and oxygen in various forms.

Analyzing the kinetics of SnO_2 thin film ozone sensor response, Korotcenkov et al. [56] have established that, for SnO_2 response and recovery processes, there were several characteristic activation energies as well. It was found that transient processes with activation energies of ~0.6–0.75 eV were typical in a wet atmosphere in the region of maximum sensitivity (T_{oper} ~ 200–300°C) (see Figure 28). The temperature dependence of the time constants for the recovery process generally showed activation energies in the range of 0.75–1.1 eV. In a dry atmosphere, the activation energies for dependence $\tau = f(1/kT)$ increased and attained 0.95–1.1 eV and 1.1–1.6 eV for the response and recovery processes, respectively. For some samples, in $\tau = f(1/kT)$ dependences, there were regions with activation energies of ~0.26–0.4 eV. As shown in Figure 28, processes with activation energies of 0.25–0.4 eV were observed at temperatures of T_{oper} < 200°C corresponding to the region of low sensitivity, while processes with activation energies of >1.0 eV generally appeared in the region of $S(T_{oper})$ dependency (T_{oper} > 300°C), which corresponds to a drop in sensor response to ozone. It is necessary to note that the change of activation energies of $\tau = f(1/kT)$ dependencies in the wide range from 0.25 to 1.6 eV demonstrates that, even for reactions of ozone detection, one should take into account the presence of various processes and reaction steps in a complex mechanism of response [224].

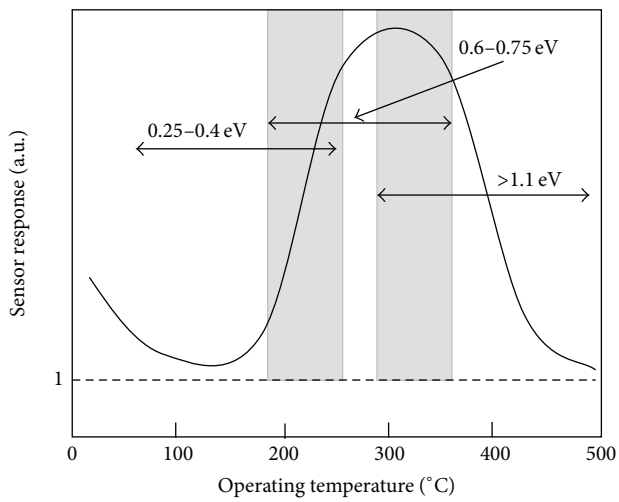

Figure 28: Diagram illustrating interrelation between temperature dependence of SnO_2 response to ozone and activation energies determined from the temperature dependence of time constants for the transient response observations. Reprinted with permission from [56]. Copyright 2007 Elsevier.

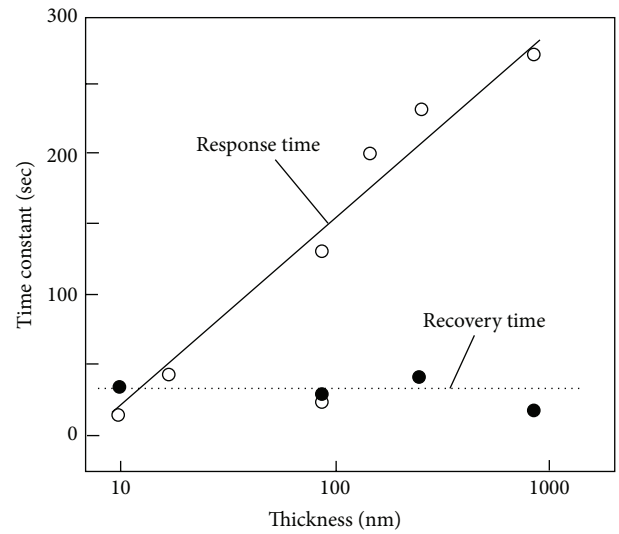

Figure 29: Response and recovery times of RT sensor response to ozone in dependence on the layer thickness. Nanoparticle In_2O_3 layer was grown at a substrate temperature of 200°C. Photoreduction was carried out using UV LED (375 nm). Adapted with permission from [176]. Copyright 2007 American Institute of Physics.

It is interesting that the activation energies reported herein are similar to those obtained during the analysis of the kinetics of SnO_2 sensor response to reducing gases [116, 211, 212]. According to [123], the processes with activation energies of 0.25–0.4 eV are the consequence of the adsorption/desorption of molecular oxygen, while the processes with activation energies of ~0.6–0.7 eV are connected to the adsorption/desorption of water, and processes with activation energies of ~1.0–1.5 eV are related to the adsorption/desorption of chemisorbed oxygen [141, 199].

7.2. RT Ozone Sensors Activated by UV Illumination. Regarding the kinetics of the response of sensors operating at room temperature, the available information is not enough for any reliable conclusions. The differences in film thicknesses, conditions of experiments, and the wavelengths and intensities of the illumination used to activate the low temperature sensitivity to ozone do not allow comparing the results obtained by different teams and making any generalizations. In addition, the presence of water greatly complicates the mechanism of ozone interaction with the surface of metal oxides. We can only refer to the results presented in [176], which showed that the effect of film thickness on the time constants of transient processes is very similar to the regularities previously established for heated sensors working in dry air [43, 44]. As for the heated sensor the response time increases with increasing film thickness, and the recovery time does not depend on the thickness (see Figure 29). These results suggest that, similar to heated sensors, the response of RT sensors activated by UV radiation is controlled by diffusion processes, whereas some kind of surface reactions, controlled by the rate of charge carrier generation by UV light, is responsible for the rate of recovery processes. In most cases, when the UV illumination has a sufficient power and film is thin, the recovery is fast and the recovery time does not exceed several tens of seconds [169, 177]. If the rate of charge carrier generation is low, the time for ozone desorption by UV irradiation can reach tens of minutes or more [177]. As a rule, this situation occurs when the film is thick or illumination with nonoptimal wavelength ($\lambda > 400$ nm) is used for activation. In this case to achieve a noticeable effect the intensity of illumination should be much greater (see Figure 30).

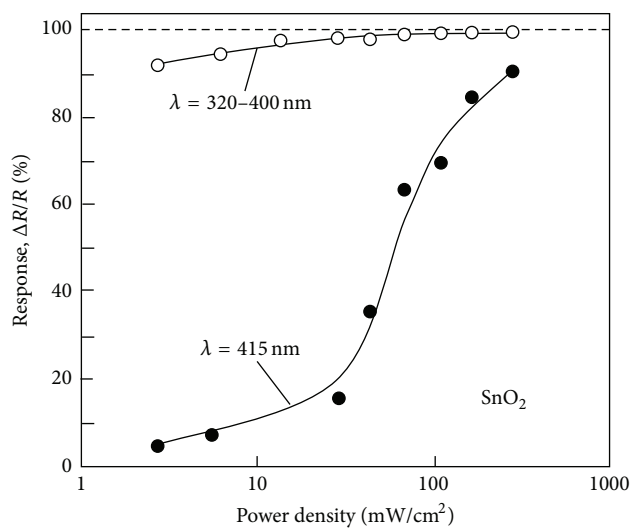

Figure 30: Dependences of the "light on" conductivity response of SnO_2 nanowires on incident power density and wavelength at room temperature. Data extracted from [186].

According to Wang et al. [176], in case of sensor response, the surface effect becomes dominant only when the film thickness decreases to 10 nm. Wang et al. [176] believe that diffusion process, which was mentioned above, is the diffusion of oxygen molecules into the layer. From our point of view, the intergrain diffusion, which was discussed in the previous section, is a more probable diffusion process. With regard to the reduction of response time with increasing ozone concentration (see Figure 16), the process is quite natural, because the rate of oxidation is directly related to the concentration of the oxidizing agent involved in the process.

8. Conclusions

This paper presents a critical assessment of the recent literature on ozone measurement with conductometric metal oxide gas sensors. The pertinent literature analysis reveals that SnO_2 and In_2O_3 metal oxides are promising materials for ozone detection in various applications. It has been shown that SnO_2- and In_2O_3-based ozone sensors can achieve excellent detection limits down to a few ppb of ozone and fast response times of approximately several seconds at optimal operation temperatures. Therefore, we believe that these metal oxides, especially In_2O_3, which has a shorter recovery time, are good choices for fabricating low-cost, low-power, highly sensitive, and fast ozone sensors aimed for the sensor market.

This work also demonstrated that ozone sensors based on SnO_2 and In_2O_3 are complex devices, and understanding their operation requires the consideration of all factors that influence final sensor performance, including surface chemical reactions, various diffusion processes, and the associated charge transfers. In the present review, we discussed these processes. However, it should be recognized that the level of understanding of these processes (i.e., the nature and origin of the mechanism that takes place between SnO_2 and In_2O_3 surfaces and ozone) is still insufficient and further research in this area is required.

We hope that the present overview of the present state of the SnO_2 and In_2O_3 response to ozone will be of interest to gas sensor developers and persuade them to carry out much more systematic research in order to better understand SnO_2 and In_2O_3 chemistry, the adsorption/desorption processes taking place at the surface of SnO_2 and In_2O_3 films with different crystallographic structures and stoichiometry, and the metal oxide-ozone interaction in atmospheres with different air humidity. Certainly, some precise theoretical calculations and computational modeling of ozone interactions with the SnO_2 and In_2O_3 surfaces and the subsequent changes in the electronic band structure of gas-adsorbed metal oxide nanostructures are required as well. We believe that deeper knowledge of physical and chemical phenomena that take place at the surface of SnO_2 and In_2O_3 can improve the sensing capabilities of these sensing materials for real applications.

Competing Interests

The authors declare that they have no competing interests.

Acknowledgments

This work was supported by the Ministry of Science, ICT and Future Planning of Korea via KOFST and NRF Programs and Grants (nos. 2011-0028736 and 2013-K000315) and partly by the Moldova Government under Grant 15.817.02.29F and ASM-STCU Project no. 5937.

References

[1] R. G. Rice and A. Netzer, *Handbook of Ozone Technology and Applications*, Ann Arbor Science, Ann Arbor, Mich, USA, 1984.

[2] P. Siesverda, "A review of ozone applications in public aquaria," in *Proceedings of the 9th Ozone World Congress*, pp. 246–295, New York, NY, USA, 1989.

[3] V. Camel and A. Bermond, "The use of ozone and associated oxidation processes in drinking water treatment," *Water Research*, vol. 32, no. 11, pp. 3208–3222, 1998.

[4] M. Horvath, L. Bilitzky, and J. Hüttner, *Ozone*, Elsevier, Amsterdam, The Netherlands, 1985.

[5] G. A. Cook, "Industrial uses of ozone," *Journal of Chemical Education*, vol. 59, no. 5, pp. 392–394, 1982.

[6] Applications and uses for ozone, http://o3ozone.com/q&a_informed/ozone_applications.htm.

[7] Ozone applications, Ozone solutions, Inc, http://www.ozonesolutions.com/.

[8] V. Bocci, *Ozone: A New Medical Drug*, Springer, Dordrecht, The Netherlands, 2005.

[9] C. Gottschak, J. A. Libra, and A. Saupe, *Ozonation of Water and Waste Water: A Practical Guide to Understanding Ozone and its Applications*, John Wiley & Sons, Weinheim, Germany, 2nd edition, 2010.

[10] C. O'Donnell, B. K. Tiwari, P. J. Cullen, and R. G. Rice, Eds., *Ozone in Food Processing*, John Wiley & Sons, Chichester, UK, 2012.

[11] M. D. Rowe, K. M. Novak, and P. D. Moskowitz, "Health effects of oxidants," *Environment International*, vol. 9, no. 6, pp. 515–528, 1983.

[12] N. Alexis, C. Barnes, I. L. Bernstein et al., "Health effects of air pollution," *Journal of Allergy and Clinical Immunology*, vol. 114, no. 5, pp. 1116–1123, 2004.

[13] WHO, *Air Quality Guidelines—Global Update 2005*, WHO Regional Publications, European Series, World Health Organization, Regional Office for Europe, Copenhagen, Denmark, 2006.

[14] D. Sauter, U. Weimar, G. Noetzel, J. Mitrovics, and W. Göpel, "Development of modular ozone sensor system for application in practical use," *Sensors and Actuators B: Chemical*, vol. 69, no. 1, 9 pages, 2000.

[15] C. Wang, *Metal organic chemical vapor deposition of indium oxide for ozone sensing [Ph.D. thesis]*, Albert-Ludwigs-Universität Freiburg, Freiburg, Germany, 2009.

[16] G. Korotcenkov and B. K. Cho, "Ozone measuring: what can limit application of SnO_2-based conductometric gas sensors?" *Sensors and Actuators B: Chemical*, vol. 161, no. 1, pp. 28–44, 2012.

[17] M. David, M. H. Ibrahim, S. M. Idrus et al., "Progress in ozone sensors performance: a review," *Jurnal Teknologi*, vol. 73, no. 6, pp. 23–29, 2015.

[18] G. Korotcenkov and V. Sysoev, "Conductometric metal oxide gas sensors," in *Chemical Sensors: Comprehensive Sensor Technologies*, G. Korotcenkov, Ed., vol. 4 of *Solid State Devices*, pp. 39–186, Momentum Press, New York, NY, USA, 2011.

[19] G. Korotcenkov, "Metal oxides for solid-state gas sensors: what determines our choice?" *Materials Science and Engineering B*, vol. 139, no. 1, pp. 1–23, 2007.

[20] G. M. Hansford, R. A. Freshwater, R. A. Bosch et al., "A low cost instrument based on a solid state sensor for balloon-borne atmospheric O_3 profile sounding," *Journal of Environmental Monitoring*, vol. 7, no. 2, pp. 158–162, 2005.

[21] F. Röck, N. Barsan, and U. Weimar, "Electronic nose: current status and future trends," *Chemical Reviews*, vol. 108, no. 2, pp. 705–725, 2008.

[22] G. Korotcenkov and J. R. Stetter, "Chemical gas mixture analysis and the electronic nose: current status, future trends," in *Chemical Sensors: Comprehensive Sensor Technologies*, G. Korotcenkov, Ed., vol. 6 of *Chemical Sensors Applications*, pp. 1–56, Momentum Press, New York, NY, USA, 2011.

[23] M. Bart, D. E. Williams, B. Ainslie et al., "High density ozone monitoring using gas sensitive semi-conductor sensors in the lower Fraser valley, British Columbia," *Environmental Science and Technology*, vol. 48, no. 7, pp. 3970–3977, 2014.

[24] N. Barsan and U. Weimar, "Conduction model of metal oxide gas sensors," *Journal of Electroceramics*, vol. 7, no. 3, pp. 143–167, 2001.

[25] D. E. Williams, "Conduction and gas response of semiconductor gas sensors," in *Solid State Gas Sensors*, P. T. Moseley and B. C. Tofield, Eds., pp. 71–123, Taylor and Francis, Bristol, Pa, USA, 1987.

[26] M. J. Madou and S. R. Morrison, *Chemical Sensing with Solid State Devices*, Academic Press, New York, NY, USA, 1989.

[27] S. R. Morrison, *The Chemical Physics of Surfaces*, Plenum, New York, NY, USA, 2nd edition, 1990.

[28] V. Brynzari, G. Korotchenkov, and S. Dmitriev, "Theoretical study of semiconductor thin film gas sensitivity: attempt to consistent approach," *Journal of Electronic Technology*, vol. 33, pp. 225–235, 2000.

[29] N. Bârsan and U. Weimar, "Understanding the fundamental principles of metal oxide based gas sensors; the example of CO sensing with SnO_2 sensors in the presence of humidity," *Journal of Physics Condensed Matter*, vol. 15, no. 20, pp. R813–R839, 2003.

[30] I.-D. Kim, A. Rothschild, and H. L. Tuller, "Advances and new directions in gas-sensing devices," *Acta Materialia*, vol. 61, no. 3, pp. 974–1000, 2013.

[31] V. Krivetskiy, M. Rumyantseva, and A. Gaskov, "Design, synthesis and application of metal oxide based sensing elements: a chemical principles approach," in *Metal Oxide Nanomaterials for Chemical Sensors*, M. A. Carpenter, S. Mathur, and A. Kolmakov, Eds., pp. 69–118, Springer Science, Business Media, New York, NY, USA, 2013.

[32] G. Korotcenkov, *Handbook of Gas Sensor Materials*, vol. 1-2, Springer, New York, NY, USA, 2013.

[33] T. Sahm, A. Gurlo, N. Bârsan, and U. Weimar, "Properties of indium oxide semiconducting sensors deposited by different techniques," *Particulate Science and Technology*, vol. 24, no. 4, pp. 441–452, 2006.

[34] T. V. Belysheva, G. N. Gerasimov, V. F. Gromov, L. I. Trachtenber, and T. V. Belysheva, "The sensor properties of Fe_2O_3-In_2O_3 films: ozone detection in air in the range of low concentration," *Russian Journal of Physical Chemistry A: Focus on Chemistry*, vol. 82, no. 10, pp. 1721–1725, 2008.

[35] T. K. H. Starke and G. S. V. Coles, "High sensitivity ozone sensors for environmental monitoring produced using laser ablated nanocrystalline metal oxides," *IEEE Sensors Journal*, vol. 2, no. 1, pp. 14–19, 2002.

[36] M. Ivanovskaya, "Ceramic and film metaloxide sensors obtained by sol-gel method: structural features and gas-sensitive properties," *Electron Technology*, vol. 33, no. 1, pp. 108–113, 2000.

[37] G. Korotcenkov, "Gas response control through structural and chemical modification of metal oxide films: state of the art and approaches," *Sensors and Actuators B: Chemical*, vol. 107, no. 1, pp. 209–232, 2005.

[38] N. Katsarakis, M. Bender, V. Cimalla, and E. Gagaoudakis, "Ozone sensing properties of DC-sputtered, c-axis oriented ZnO films at room temperature," *Sensors and Actuators B: Chemical*, vol. 96, no. 1-2, pp. 76–81, 2003.

[39] S. R. Utembe, G. M. Hansford, M. G. Sanderson et al., "An ozone monitoring instrument based on the tungsten trioxide (WO_3) semiconductor," *Sensors and Actuators B: Chemical*, vol. 114, no. 1, pp. 507–512, 2006.

[40] A. Labidi, E. Gillet, R. Delamare, M. Maaref, and K. Aguir, "Ethanol and ozone sensing characteristics of WO_3 based sensors activated by Au and Pd," *Sensors and Actuators B: Chemical*, vol. 120, no. 1, pp. 338–345, 2006.

[41] L. A. Obvintseva, "Metal oxide semiconductor sensors for determination of reactive gas impurities in air," *Russian Journal of General Chemistry*, vol. 78, no. 12, pp. 2545–2555, 2008.

[42] M. Ivanovskaya, A. Gurlo, and P. Bogdanov, "Mechanism of O_3 and NO_2 detection and selectivity of In_2O_3 sensors," *Sensors and Actuators, B: Chemical*, vol. 77, no. 1-2, pp. 264–267, 2001.

[43] G. Korotcenkov, V. Brinzari, A. Cerneavschi et al., "The influence of film structure on In_2O_3 gas response," *Thin Solid Films*, vol. 460, no. 1-2, pp. 315–323, 2004.

[44] G. Korotcenkov, A. Cerneavschi, V. Brinzari et al., "In_2O_3 films deposited by spray pyrolysis as a material for ozone gas sensors," *Sensors and Actuators B: Chemical*, vol. 99, no. 2-3, pp. 297–303, 2004.

[45] G. Korotcenkov, I. Blinov, M. Ivanov, and J. R. Stetter, "Ozone sensors on the base of SnO_2 films deposited by spray pyrolysis," *Sensors and Actuators B: Chemical*, vol. 120, no. 2, pp. 679–686, 2007.

[46] C. Baratto, M. Ferroni, G. Faglia, and G. Sberveglieri, "Iron-doped indium oxide by modified RGTO deposition for ozone sensing," *Sensors and Actuators B: Chemical*, vol. 118, no. 1-2, pp. 221–225, 2006.

[47] G. Korotcenkov, V. Macsanov, V. Tolstoy, V. Brinzari, J. Schwank, and G. Fagila, "Structural and gas response characterization of nano-size SnO_2 films deposited by SILD method," *Sensors and Actuators B: Chemical*, vol. 96, no. 3, pp. 602–609, 2003.

[48] O. Korostynska, K. Arshak, G. Hickey, and E. Forde, "Ozone and gamma radiation sensing properties of In_2O_3:ZnO:SnO_2 thin films," *Microsystem Technologies*, vol. 14, no. 4-5, pp. 557–566, 2008.

[49] J.-B. Sun, J. Xu, B. Wang, P. Sun, F.-M. Liu, and G.-Y. Lu, "UV-enhanced room temperature ozone sensor based on hierarchical SnO_2-In_2O_3," *Chemical Research in Chinese Universities*, vol. 28, no. 3, pp. 483–487, 2012.

[50] M. Epifani, E. Comini, J. Arbiol et al., "Chemical synthesis of In_2O_3 nanocrystals and their application in highly performing ozone-sensing devices," *Sensors and Actuators B: Chemical*, vol. 130, no. 1, pp. 483–487, 2008.

[51] M. Epifani, S. Capone, R. Rella et al., "In_2O_3 thin films obtained through a chemical complexation based sol-gel process and their application as gas sensor devices," *Journal of Sol-Gel Science and Technology*, vol. 26, no. 1–3, pp. 741–744, 2003.

[52] A. Oprea, A. Gurlo, N. Bârsan, and U. Weimar, "Transport and gas sensing properties of In_2O_3 nanocrystalline thick films: a Hall effect based approach," *Sensors and Actuators B: Chemical*, vol. 139, no. 2, pp. 322–328, 2009.

[53] G. Korotcenkov, M. Ivanov, I. Blinov, and J. R. Stetter, "Kinetics of indium oxide-based thin film gas sensor response: the role of 'redox' and adsorption/desorption processes in gas sensing effects," *Thin Solid Films*, vol. 515, no. 7-8, pp. 3987–3996, 2007.

[54] G. Korotcenkov, V. Brinzari, J. R. Stetter, I. Blinov, and V. Blaja, "The nature of processes controlling the kinetics of indium oxide-based thin film gas sensor response," *Sensors and Actuators B: Chemical*, vol. 128, no. 1, pp. 51–63, 2007.

[55] T. Takada, K. Suzuki, and M. Nakane, "Highly sensitive ozone sensor," *Sensors and Actuators B: Chemical*, vol. 13, no. 1-3, pp. 404–407, 1993.

[56] G. Korotcenkov, I. Blinov, V. Brinzari, and J. R. Stetter, "Effect of air humidity on gas response of SnO_2 thin film ozone sensors," *Sensors and Actuators B: Chemical*, vol. 122, no. 2, pp. 519–526, 2007.

[57] G. Korotcenkov and B. K. Cho, "Thin film SnO_2-based gas sensors: film thickness influence," *Sensors and Actuators B: Chemical*, vol. 142, no. 1, pp. 321–330, 2009.

[58] L. Berry and J. Brunet, "Oxygen influence on the interaction mechanisms of ozone on SnO_2 sensors," *Sensors and Actuators, B: Chemical*, vol. 129, no. 1, pp. 450–458, 2008.

[59] V. Demarne and A. Grisel, "A new SnO_2 low temperature deposition technique for integrated gas sensors," *Sensors and Actuators B: Chemical*, vol. 15, no. 1–3, pp. 63–67, 1993.

[60] Th. Becker, L. Tomasi, C. B.-V. Braunmühl et al., "Ozone detection using low-power-consumption metal-oxide gas sensors," *Sensors and Actuators A: Physical*, vol. 74, no. 1–3, pp. 229–232, 1999.

[61] W. Hellmich, C. B.-V. Braunmühl, G. Müller, G. Sberveglieri, M. Berti, and C. Perego, "The kinetics of formation of gas-sensitive RGTO-SnO_2 films," *Thin Solid Films*, vol. 263, no. 2, pp. 231–237, 1995.

[62] G. Korotcenkov, B. K. Cho, L. Gulina, and V. Tolstoy, "Ozone sensors based on SnO_2 films modified by SnO_2-Au nanocomposites synthesized by the SILD method," *Sensors and Actuators, B: Chemical*, vol. 138, no. 2, pp. 512–517, 2009.

[63] C. Cantalini, W. Wlodarski, Y. Li et al., "Investigation on the O_3 sensitivity properties of WO_3 thin films prepared by sol–gel, thermal evaporation and r.f. sputtering techniques," *Sensors and Actuators B: Chemical*, vol. 64, no. 1–3, pp. 182–188, 2000.

[64] O. Berger, T. Hoffman, W.-J. Fischer, and V. Melev, "Tungsten-oxide thin films as novel materials with high sensitivity and selectivity to NO_2, O_3, and H2S. Part II: application as gas sensors," *Journal of Materials Science: Materials in Electronics*, vol. 15, no. 7, pp. 483–493, 2004.

[65] W. Belkacem, A. Labidi, J. Guérin, N. Mliki, and K. Aguir, "Cobalt nanograins effect on the ozone detection by WO_3 sensors," *Sensors and Actuators B: Chemical*, vol. 132, no. 1, pp. 196–201, 2008.

[66] J. Guérin, M. Bendahan, and K. Aguir, "A dynamic response model for the WO_3-based ozone sensors," *Sensors and Actuators B: Chemical*, vol. 128, no. 2, pp. 462–467, 2008.

[67] R. Boulmani, M. Bendahan, C. Lambert-Mauriat, M. Gillet, and K. Aguir, "Correlation between rf-sputtering parameters and WO_3 sensor response towards ozone," *Sensors and Actuators B: Chemical*, vol. 125, no. 2, pp. 622–627, 2007.

[68] A. Labidi, M. Gaidi, J. Guérin, A. Bejaoui, M. Maaref, and K. Aguir, "Alternating current investigation and modeling of the temperature and ozone effects on the grains and the grain boundary contributions to the WO_3 sensor responses," *Thin Solid Films*, vol. 518, no. 1, pp. 355–361, 2009.

[69] A. Labidi, C. Jacolin, M. Bendahan et al., "Impedance spectroscopy on WO_3 gas sensor," *Sensors and Actuators B: Chemical*, vol. 106, no. 2, pp. 713–718, 2005.

[70] J. Guérin, K. Aguir, M. Bendahan, and C. Lambert-Mauriat, "Thermal modelling of a WO_3 ozone sensor response," *Sensors and Actuators B: Chemical*, vol. 104, no. 2, pp. 289–293, 2005.

[71] A. C. Catto, L. F. da Silva, C. Ribeiro et al., "An easy method of preparing ozone gas sensors based on ZnO nanorods," *RSC Advances*, vol. 5, no. 25, pp. 19528–19533, 2015.

[72] M. Acuautla, S. Bernardini, M. Bendahan, and E. Pietri, "Thickness effects of ZnO thin films on flexible ozone sensors," in *Proceedings of 10th Conference on Research in Microelectronics and Electronics (PRIME '14)*, pp. 1–4, IEEE, Grenoble, France, June 2014.

[73] K. Galatsis, Y. X. Li, W. Wlodarski et al., "Comparison of single and binary oxide MoO_3, TiO_2 and WO_3 sol-gel gas sensors," *Sensors and Actuators B: Chemical*, vol. 83, no. 1–3, pp. 276–280, 2002.

[74] M. Debliquy, C. Baroni, A. Boudiba, J.-M. Tulliani, M. Olivier, and C. Zhang, "Sensing characteristics of hematite and barium oxide doped hematite films towards ozone and nitrogen dioxide," *Procedia Engineering*, vol. 25, pp. 219–222, 2011.

[75] Y. Hosoya, Y. Itagaki, H. Aono, and Y. Sadaoka, "Ozone detection in air using $SmFeO_3$ gas sensor," *Sensors and Actuators B: Chemical*, vol. 108, no. 1-2, pp. 198–201, 2005.

[76] T. Takada and K. Komatsu, "Ozone detection by In_2O_3 thin films gas sensor," in *Proceedings of the 4th International Conference on Solid State Sensors and Actuators*, pp. 693–696, Tokyo, Japan, June 1987.

[77] T. Takada, "Ozone detection by In_2O_3 thin films gas sensor," in *Chemical Sensor Technology. Kodansha*, T. Seiyama, Ed., vol. 2, pp. 59–70, Elsevier, Tokyo, Japan, 1989.

[78] D. F. Cox, T. B. Fryberger, and S. Semancik, "Oxygen vacancies and defect electronic states on the $SnO_2(110)$-1×1 surface," *Physical Review B*, vol. 38, pp. 2072–2083, 1988.

[79] K. Tabata, T. Kawabe, Y. Yamaguchi, and Y. Nagasawa, "Chemisorbed oxygen species over the (110) face of SnO_2," *Catalysis Surveys from Asia*, vol. 7, no. 4, pp. 251–259, 2003.

[80] P. Agoston, *Point defect and surface properties of In_2O_3 and SnO_2: a comparative study by first-principles methods [Ph.D. thesis]*, Technische Universität Darmstadt, Darmstadt, Germany, 2011.

[81] Th. Becker, S. Ahlers, C. Bosch-v Braunmühl, G. Muller, and O. Kiesewetter, "Gas sensing properties of thin- and thick-film tin-oxide materials," *Sensors and Actuators B: Chemical*, vol. 77, no. 1-2, pp. 55–61, 2001.

[82] S.-R. Kim, H.-K. Hong, C. H. Kwon, D. H. Yun, K. Lee, and Y. K. Sung, "Ozone sensing properties of In_2O_3-based semiconductor thick films," *Sensors and Actuators B: Chemical*, vol. 66, no. 1, pp. 59–62, 2000.

[83] W. Gopel, "Chemisorption and charge transfer at ionic semiconductor surfaces: implications in designing gas sensors," *Progress in Surface Science*, vol. 20, no. 1, pp. 9–103, 1985.

[84] M. Egashira, "An overview on semiconductor gas sensors," in *Proceedings of the Symposium on Chemical Sensors and Proceedings of the Electrochemical Society (ECS '87)*, D. R. Turner, Ed., vol. 87–89, pp. 39–48, Pennington, NJ, USA, 1987.

[85] G. Sberveglieri, Ed., *Gas Sensors*, Kluwer Academic Publishers, Dordrecht, The Netherlands, 1992.

[86] N. Barsan, M. Schweizer-Berberich, and W. Göpel, "Fundamental and practical aspects in the design of nanoscaled SnO_2 gas sensors: a status report," *Fresenius' Journal of Analytical Chemistry*, vol. 365, no. 4, pp. 287–304, 1999.

[87] W. Gopel and G. Reinhardt, "Metal oxide sensors: new devices through tailoring interfaces on the atomic scale," in *Sensors Update. Sensor Technology—Applications Markets*, H. Baltes, W. Gopel, and J. Hesse, Eds., vol. 1, pp. 49–120, VCH Publishers, Weinheim, Germany, 1996.

[88] A. Gurlo, N. Barsan, and U. Weimar, "Gas sensors based on semiconducting metal oxides," in *Metal Oxides: Chemistry and Applications*, J. L. G. Fierro, Ed., Marcel Dekker, New York, NY, USA, 2004.

[89] E. Comini, G. Faglia, and G. Sberveglieri, Eds., *Solid State Gas Sensing*, Springer, New York, NY, USA, 2009.

[90] G. Korotcenkov, V. Brinzari, A. Cerneavschi et al., "In_2O_3 films deposited by spray pyrolysis: gas response to reducing (CO, H_2) gases," *Sensors and Actuators B: Chemical*, vol. 98, no. 2-3, pp. 122–129, 2004.

[91] T. Doll, A. Fuchs, I. Eisele, G. Faglia, S. Groppelli, and G. Sberveglieri, "Conductivity and work function ozone sensors based on indium oxide," *Sensors and Actuators B: Chemical*, vol. 49, no. 1-2, pp. 63–67, 1998.

[92] V. R. Mastelaro, S. C. Zílio, L. F. da Silva et al., "Ozone gas sensor based on nanocrystalline $SrTi_{1-x}Fe_xO_3$ thin films," *Sensors and Actuators B: Chemical*, vol. 181, pp. 919–924, 2013.

[93] A. Bejaoui, J. Guerin, J. A. Zapien, and K. Aguir, "Theoretical and experimental study of the response of CuO gas sensor under ozone," *Sensors and Actuators B: Chemical*, vol. 190, pp. 8–15, 2014.

[94] L. F. da Silva, A. C. Catto, W. Avansi Jr. et al., "A novel ozone gas sensor based on one-dimensional (1D) α-Ag_2WO_4 nanostructures," *Nanoscale*, vol. 6, no. 8, pp. 4058–4062, 2014.

[95] G. Korotcenkov, V. Golovanov, V. Brinzari, A. Cornet, J. Morante, and M. Ivanov, "Distinguishing feature of metal oxide films' structural engineering for gas sensor applications," *Journal of Physics: Conference Series*, vol. 15, no. 1, pp. 256–261, 2005.

[96] A. Walsh and C. R. A. Catlow, "Structure, stability and work functions of the low index surfaces of pure indium oxide and Sn-doped indium oxide (ITO) from density functional theory," *Journal of Materials Chemistry*, vol. 20, no. 46, pp. 10438–10444, 2010.

[97] G. Korotcenkov, "The role of morphology and crystallographic structure of metal oxides in response of conductometric-type gas sensors," *Materials Science and Engineering R: Reports*, vol. 61, no. 1–6, pp. 1–39, 2008.

[98] G. Korotcenkov and B. K. Cho, "The role of grain size on the thermal instability of nanostructured metal oxides used in gas sensor applications and approaches for grain-size stabilization," *Progress in Crystal Growth and Characterization of Materials*, vol. 58, no. 4, pp. 167–208, 2012.

[99] G. Korotcenkov, A. Cornet, E. Rossinyol, J. Arbiol, V. Brinzari, and Y. Blinov, "Faceting characterization of tin dioxide nanocrystals deposited by spray pyrolysis from stannic chloride water solution," *Thin Solid Films*, vol. 471, no. 1-2, pp. 310–319, 2005.

[100] G. Korotcenkov, M. Dibattista, J. Schwank, and V. Brinzari, "Structural characterization of SnO_2 gas sensing films deposited by spray pyrolysis," *Materials Science and Engineering B*, vol. 77, no. 1, pp. 33–39, 2000.

[101] G. Korotcenkov, A. Cerneavschi, V. Brinzari et al., "Crystallographic characterization of In_2O_3 films deposited by spray pyrolysis," *Sensors and Actuators B: Chemical*, vol. 84, no. 1, pp. 37–42, 2002.

[102] G. Korotcenkov, V. Brinzari, M. Ivanov et al., "Structural stability of indium oxide films deposited by spray pyrolysis during thermal annealing," *Thin Solid Films*, vol. 479, no. 1-2, pp. 38–51, 2005.

[103] P. Agoston and K. Albe, "Thermodynamic stability, stoichiometry, and electronic structure of bcc-In_2O_3 surfaces," *Physical Review B*, vol. 84, no. 4, Article ID 045311, 2011.

[104] K. H. L. Zhang, A. Walsh, C. R. A. Catlow, V. K. Lazarov, and R. G. Egdell, "Surface energies control the self-organization of oriented In_2O_3 nanostructures on cubic zirconia," *Nano Letters*, vol. 10, no. 9, pp. 3740–3746, 2010.

[105] M. Batzill and U. Diebold, "The surface and materials science of tin oxide," *Progress in Surface Science*, vol. 79, no. 2–4, pp. 47–154, 2005.

[106] C. Xu, J. Tamaki, N. Miura, and N. Yamazoe, "Grain size effects on gas sensitivity of porous SnO_2-based elements," *Sensors and Actuators B: Chemical*, vol. 3, no. 2, pp. 147–155, 1991.

[107] X. Wang, S. S. Yee, and W. P. Carey, "Transition between neck controlled and grain-boundary-controlled sensitivity of metal oxide gas sensors," *Sensors and Actuators B: Chemical*, vol. 25, no. 1–3, pp. 454–457, 1995.

[108] A. Rothschild and Y. Komem, "The effect of grain size on the sensitivity of nanocrystalline metal-oxide gas sensors," *Journal of Applied Physics*, vol. 95, no. 11, pp. 6374–6380, 2004.

[109] G. Korotcenkov, S. D. Han, B. K. Cho, and V. Brinzari, "Grain size effects in sensor response of nanostructured SnO_2- and In_2O_3-based conductometric gas sensor," *Critical Reviews in Solid State and Materials Sciences*, vol. 34, no. 1-2, pp. 1–17, 2009.

[110] Y. Hao, G. Meng, C. Ye, and L. Zhang, "Controlled synthesis of In_2O_3 octahedrons and nanowires," *Crystal Growth and Design*, vol. 5, no. 4, pp. 1617–1621, 2005.

[111] M. Shi, F. Xu, K. Yu, Z. Zhu, and J. Fang, "Controllable synthesis of In_2O_3 nanocubes, truncated nanocubes, and symmetric multipods," *Journal of Physical Chemistry C*, vol. 111, no. 44, pp. 16267–16271, 2007.

[112] A. Gurlo, "Nanosensors: towards morphological control of gas sensing activity. SnO_2, In_2O_3, ZnO and WO_3 case studies," *Nanoscale*, vol. 3, no. 1, pp. 154–165, 2011.

[113] G. Korotcenkov, S. H. Han, and B. K. Cho, "Material design for metal oxide chemiresistive gas sensors," *Journal of Sensor Science and Technology*, vol. 22, no. 1, pp. 1–17, 2013.

[114] V. Brinzari, G. Korotcenkov, J. Schwank, V. Lantto, S. Saukko, and V. Golovanov, "Morphological rank of nano-scale tin dioxide films deposited by spray pyrolysis from $SnCl_4 \bullet 5H_2O$ water solution," *Thin Solid Films*, vol. 408, no. 1-2, pp. 51–58, 2002.

[115] G. Korotcenkov, I. Boris, A. Cornet et al., "The influence of additives on gas sensing and structural properties of In_2O_3-based ceramics," *Sensors and Actuators B: Chemical*, vol. 120, no. 2, pp. 657–664, 2007.

[116] G. Korotcenkov, V. Brinzari, V. Golovanov, and Y. Blinov, "Kinetics of gas response to reducing gases of SnO_2 films, deposited by spray pyrolysis," *Sensors and Actuators B: Chemical*, vol. 98, no. 1, pp. 41–45, 2004.

[117] I. Lundström, "Approaches and mechanisms to solid state based sensing," *Sensors and Actuators B: Chemical*, vol. 35, no. 1–3, pp. 11–19, 1996.

[118] A. Gurlo, N. Barsan, U. Weimar, M. Ivanovskaya, A. Taurino, and P. Siciliano, "Polycrystalline well-shaped blocks of indium oxide obtained by the sol-gel method and their gas-sensing properties," *Chemistry of Materials*, vol. 15, no. 23, pp. 4377–4383, 2003.

[119] T. Wagner, J. Hennemann, C.-D. Kohl, and M. Tiemann, "Photocatalytic ozone sensor based on mesoporous indium oxide: influence of the relative humidity on the sensing performance," *Thin Solid Films*, vol. 520, no. 3, pp. 918–921, 2011.

[120] T. Takada, H. Tanjou, T. Saito, and K. Harada, "Aqueous ozone detector using In_2O_3 thin-film semiconductor gas sensor," *Sensors and Actuators B: Chemical*, vol. 24-25, no. 1–3, pp. 548–551, 1995.

[121] C. Y. Wang, S. Bagchi, M. Bitterling et al., "Photon stimulated ozone sensor based on indium oxide nanoparticles II: ozone monitoring in humidity and water environments," *Sensors and Actuators B: Chemical*, vol. 164, no. 1, pp. 37–42, 2012.

[122] A. Hattori, H. Tachibana, N. Yoshiike, and A. Yoshida, "Ozone sensor made by dip coating method," *Sensors and Actuators A: Physical*, vol. 77, no. 2, pp. 120–125, 1999.

[123] A. Gurlo, N. Barsan, M. Ivanovskaya, U. Weimar, and W. Gopel, "In_2O_3 and MoO_3–In_2O_3 thin film semiconductor sensors: interaction with NO_2 and O_3," *Sensors and Actuators B: Chemical*, vol. 47, no. 1, pp. 92–99, 1998.

[124] J. Frank, M. Fleischer, M. Zimmer, and H. Meixner, "Ozone sensing using In_2O_3-modified Ga_2O_3 thin films," *IEEE Sensors Journal*, vol. 1, no. 4, pp. 318–321, 2001.

[125] P. K. Clifford and D. T. Tuma, "Characteristics of semiconductor gas sensors I. Steady state gas response," *Sensors and Actuators*, vol. 3, pp. 233–254, 1982.

[126] S. Strässler and A. Reis, "Simple models for N-type metal oxide gas sensors," *Sensors and Actuators*, vol. 4, pp. 465–472, 1983.

[127] S. R. Morrison, "Mechanism of semiconductor gas sensor operation," *Sensors and Actuators*, vol. 11, no. 3, pp. 283–287, 1987.

[128] J. F. McAleer, P. T. Moseley, J. O. W. Norris, and D. E. Williams, "Tin dioxide gas sensors. Part 1.—aspects of the surface chemistry revealed by electrical conductance variations," *Journal of the Chemical Society, Faraday Transactions 1: Physical Chemistry in Condensed Phases*, vol. 83, no. 4, pp. 1323–1346, 1987.

[129] D. E. Williams and K. F. E. Pratt, "Microstructure effects on the response of gas-sensitive resistors based on semiconducting oxides," *Sensors and Actuators B: Chemical*, vol. 70, no. 1–3, pp. 214–221, 2000.

[130] G. Chabanis, I. P. Parkin, and D. E. Williams, "A simple equivalent circuit model to represent microstructure effects on the response of semiconducting oxide-based gas sensors," *Measurement Science and Technology*, vol. 14, no. 1, pp. 76–86, 2003.

[131] V. Brinzari, M. Ivanov, B. K. Cho, M. Kamei, and G. Korotcenkov, "Photoconductivity in In_2O_3 nanoscale thin films: interrelation with chemisorbed-type conductometric response towards oxygen," *Sensors and Actuators B: Chemical*, vol. 148, no. 2, pp. 427–438, 2010.

[132] G. Munuera, V. Rives-Arnau, and A. Saucedo, "Photo-adsorption and photo-desorption of oxygen on highly hydroxylated TiO_2 surfaces. Part 1.—role of hydroxyl groups in photo-adsorption," *Journal of the Chemical Society, Faraday Transactions 1*, vol. 75, pp. 736–747, 1979.

[133] D. E. Williams, S. R. Aliwell, K. F. E. Pratt et al., "Modelling the response of a tungsten oxide semiconductor as a gas sensor for the measurement of ozone," *Measurement Science and Technology*, vol. 13, no. 6, pp. 923–931, 2002.

[134] J. Guérin, K. Aguir, and M. Bendahan, "Modeling of the conduction in a WO_3 thin film as ozone sensor," *Sensors and Actuators B: Chemical*, vol. 119, no. 1, pp. 327–334, 2006.

[135] V. V. Lunin, M. P. Popovich, and S. N. Tkachenko, *Physical Chemistry of Ozone*, Moscow State University, Moscow, Russia, 1998 (Russian).

[136] K. M. Bulanin, J. C. Lavalley, and A. A. Tsyganenko, "Infrared study of ozone adsorption on TiO_2 (anatase)," *Journal of Physical Chemistry*, vol. 99, no. 25, pp. 10294–10298, 1995.

[137] B. Dhandapani and S. T. Oyama, "Gas phase ozone decomposition catalysts," *Applied Catalysis B: Environmental*, vol. 11, no. 2, pp. 129–166, 1997.

[138] A. Banichevich, S. D. Peyerimhoff, and F. Grein, "Ab initio potential surfaces for ozone dissociation in its ground and various electronically excited states," *Chemical Physics Letters*, vol. 173, no. 1, pp. 1–6, 1990.

[139] M. Allan, K. R. Asmis, D. B. Popovic, M. Stepanovic, N. J. Mason, and J. A. Davies, "Production of vibrationally autodetaching O_2- in low-energy electron impact on ozone," *Journal of Physics B: Atomic, Molecular and Optical Physics*, vol. 29, no. 15, pp. 3487–3495, 1996.

[140] A. Naydenov, R. Stoyanova, and D. Mehandjiev, "Ozone decomposition and CO oxidation on CeO_2," *Journal of Molecular Catalysis A: Chemical*, vol. 98, no. 1, pp. 9–14, 1995.

[141] T. Doll, J. Lechner, I. Eisele, K.-D. Schierbaum, and W. Göpel, "Ozone detection in the ppb range with work function sensors operating at room temperature," *Sensors and Actuators B: Chemical*, vol. 34, no. 1–3, pp. 506–510, 1996.

[142] D. E. Williams and K. F. E. Patt, "Classification of reactive sites on the surface of polycrystalline tin dioxide," *Journal of the Chemical Society, Faraday Transactions*, vol. 94, no. 23, pp. 3493–3500, 1998.

[143] M. Calatayud, A. Markovits, M. Menetrey, B. Mguig, and C. Minot, "Adsorption on perfect and reduced surfaces of metal oxides," *Catalysis Today*, vol. 85, no. 2–4, pp. 125–143, 2003.

[144] F. Trani, M. Causà, D. Ninno, G. Cantele, and V. Barone, "Density functional study of oxygen vacancies at the SnO_2 surface and subsurface sites," *Physical Review B*, vol. 77, no. 24, Article ID 245410, 2008.

[145] A. Rothschild, Y. Komem, and F. Cosandey, "Low temperature reoxidation mechanism in nanocrystalline $TiO_{2-\delta}$ thin films thin films," *Journal of the Electrochemical Society*, vol. 148, no. 8, pp. H85–H89, 2001.

[146] J. Jamnik, B. Kamp, R. Merkle, and J. Maier, "Space charge influenced oxygen incorporation in oxides: in how far does it contribute to the drift of Taguchi sensors?" *Solid State Ionics*, vol. 150, no. 1-2, pp. 157–166, 2002.

[147] J. Fleig, R. Merkle, and J. Maier, "The $p(O_2)$ dependence of oxygen surface coverage and exchange current density of mixed conducting oxide electrodes: model considerations," *Physical Chemistry Chemical Physics*, vol. 9, no. 21, pp. 2713–2723, 2007.

[148] S. B. Adler, X. Y. Chen, and J. R. Wilson, "Mechanisms and rate laws for oxygen exchange on mixed-conducting oxide surfaces," *Journal of Catalysis*, vol. 245, no. 1, pp. 91–109, 2007.

[149] R. Merkle and J. Maier, "How is oxygen incorporated into oxides? A comprehensive kinetic study of a simple solid-state reaction with $SrTiO_3$ as a model material," *Angewandte Chemie—International Edition*, vol. 47, no. 21, pp. 3874–3894, 2008.

[150] C. Körber, A. Wachau, P. Ágoston, K. Albe, and A. Klein, "Self-limited oxygen exchange kinetics at SnO_2 surfaces," *Physical Chemistry Chemical Physics*, vol. 13, no. 8, pp. 3223–3226, 2011.

[151] M. Himmerlich, *Surface characterization of indium compounds as functional layers for (opto)electronic and sensoric applications [Ph.D. thesis]*, Technische Universität Ilmenau, Ilmenau, Germany, 2008.

[152] P. G. Harrison and M. J. Willett, "Tin oxide surfaces. Part 20.—electrical properties of tin(IV) oxide gel: nature of the surface species controlling the electrical conductance in air as a function of temperature," *Journal of the Chemical Society, Faraday Transactions 1: Physical Chemistry in Condensed Phases*, vol. 85, no. 8, pp. 1921–1932, 1989.

[153] M. Vahedpour, M. Tozihi, and F. Nazari, "Mechanistic study of ozone-water reaction and their reaction products with gas phase elemental mercury: a computational study," *Chinese Journal of Chemistry*, vol. 28, no. 7, pp. 1103–1113, 2010.

[154] V. Brinzari, G. Korotcenkov, K. Veltruska, V. Matolin, N. Tsud, and J. Schwank, "XPS study of gas sensitive SnO_2 thin films," in *Proceedings of the Semiconductor International Conference (CAS '00)*, vol. 1, pp. 127–130, Sinaia , Romania, October 2000.

[155] V. M. Bermudez, A. D. Berry, H. Kim, and A. Piqué, "Functionalization of indium tin oxide," *Langmuir*, vol. 22, no. 26, pp. 11113–11125, 2006.

[156] K. Ip, B. P. Gila, A. H. Onstine et al., "Effect of ozone cleaning on Pt/Au and W/Pt/Au Schottky contacts to n-type ZnO," *Applied Surface Science*, vol. 236, no. 1, pp. 387–393, 2004.

[157] M. Tominaga, N. Hirata, and I. Taniguchi, "UV-ozone dry-cleaning process for indium oxide electrodes for protein electrochemistry," *Electrochemistry Communications*, vol. 7, no. 12, pp. 1423–1428, 2005.

[158] M. Himmerlich, C. Y. Wang, V. Cimalla, O. Ambacher, and S. Krischok, "Surface properties of stoichiometric and defect-rich indium oxide films grown by MOCVD," *Journal of Applied Physics*, vol. 111, no. 9, Article ID 093704, 2012.

[159] F. Wolkenstein, *The Electron Theory of Catalysis on Semiconductors*, Macmillan Publishers, New York, NY, USA, 1963.

[160] T. Wolkenstein, *Electronic Processes on Semiconductor Surfaces During Chemisorption*, Springer, New York, NY, USA, 1991.

[161] M. Ó Conaire, H. J. Curran, J. M. Simmie, W. J. Pitz, and C. K. Westbrook, "A comprehensive modeling study of hydrogen oxidation," *International Journal of Chemical Kinetics*, vol. 36, no. 11, pp. 603–622, 2004.

[162] A. K. Gatin, M. V. Grishin, A. A. Kirsankin, L. I. Trakhtenberg, and B. R. Shub, "Adsorption of oxygen and hydrogen at the surface of nanostructured SnO_2 film," *Nanotechnologies in Russia*, vol. 7, no. 3-4, pp. 122–126, 2012.

[163] C. Y. Wang, R. W. Becker, T. Passow et al., "Photon stimulated sensor based on indium oxide nanoparticles I: wide-concentration-range ozone monitoring in air," *Sensors and Actuators B: Chemical*, vol. 152, no. 2, pp. 235–240, 2011.

[164] E. Gagaoudakis, M. Bender, E. Douloufakis et al., "The influence of deposition parameters on room temperature ozone sensing properties of InOx films," *Sensors and Actuators B: Chemical*, vol. 80, no. 2, pp. 155–161, 2001.

[165] M. Epifani, E. Comini, J. Arbiol et al., "Nanocrystals as very active interfaces: ultrasensitive room-temperature ozone sensors with in_2o_3 nanocrystals prepared by a low-temperature sol-gel process in a coordinating environment," *Journal of Physical Chemistry C*, vol. 111, no. 37, pp. 13967–13971, 2007.

[166] A. Gaddari, F. Berger, M. Amjoud et al., "A novel way for the synthesis of tin dioxide sol–gel derived thin films: application to O_3 detection at ambient temperature," *Sensors and Actuators B: Chemical*, vol. 176, pp. 811–817, 2013.

[167] F. Berger, B. Ghaddab, J. B. Sanchez, and C. Mavon, "Development of an ozone high sensitive sensor working at ambient temperature," *Journal of Physics: Conference Series*, vol. 307, no. 1, Article ID 012054, 2011.

[168] G. Kiriakidis, K. Moschovis, I. Kortidis, and R. Skarvelakis, "Highly sensitive InO_x ozone sensing films on flexible substrates," *Journal of Sensors*, vol. 2009, Article ID 727893, 5 pages, 2009.

[169] Ch. Y. Wang, V. Cimalla, C.-C. Roehlig et al., "A new type of highly sensitive portable ozone sensor operating at room temperature," in *Proceedings of the 5th IEEE Conference on Sensors*, pp. 81–84, EXCO, Daegu, South Korea, October 2006.

[170] G. Kiriakidis, M. Bender, N. Katsarakis et al., "Ozone sensing properties of polycrystalline indium oxide films at room temperature," *Physica Status Solidi (A)*, vol. 185, no. 1, pp. 27–32, 2001.

[171] M. Suchea, N. Katsarakis, S. Christoulakis, S. Nikolopoulou, and G. Kiriakidis, "Low temperature indium oxide gas sensors," *Sensors and Actuators B: Chemical*, vol. 118, no. 1-2, pp. 135–141, 2006.

[172] J. D. Prades, R. Jimenez-Diaz, M. Manzanares et al., "A model for the response towards oxidizing gases of photoactivated sensors based on individual SnO_2 nanowires," *Physical Chemistry Chemical Physics*, vol. 11, no. 46, pp. 10881–10889, 2009.

[173] M. Bender, N. Katsarakis, E. Gagaoudakis et al., "Dependence of the photoreduction and oxidation behavior of indium oxide films on substrate temperature and film thickness," *Journal of Applied Physics*, vol. 90, no. 10, pp. 5382–5387, 2001.

[174] M. Suchea, N. Katsarakis, S. Christoulakis, M. Katharakis, T. Kitsopoulos, and G. Kiriakidis, "Metal oxide thin films as sensing layers for ozone detection," *Analytica Chimica Acta*, vol. 573-574, pp. 9–13, 2006.

[175] D. Klaus, D. Klawinski, S. Amrehn, M. Tiemann, and T. Wagner, "Light-activated resistive ozone sensing at room temperature utilizing nanoporous In_2O_3 particles: influence of particle size," *Sensors and Actuators B: Chemical*, vol. 217, pp. 181–185, 2015.

[176] Ch. Y. Wang, V. Cimalla, Th. Kups et al., "Photoreduction and oxidation behavior of In_2O_3 nanoparticles by metal organic chemical vapor deposition," *Journal of Applied Physics*, vol. 102, no. 4, Article ID 044310, 2007.

[177] C. Y. Wang, V. Cimalla, M. Kunzer et al., "Near-UV LEDs for integrated InO-based ozone sensors," *Physica Status Solidi (C)*, vol. 7, no. 7-8, pp. 2177–2179, 2010.

[178] C.-C. Jeng, P. J. H. Chong, C.-C. Chiu et al., "A dynamic equilibrium method for the SnO_2-based ozone sensors using

UV-LED continuous irradiation," *Sensors and Actuators B: Chemical*, vol. 195, pp. 702–706, 2014.

[179] S. Mills, M. Lim, B. Lee, and V. Misra, "Atomic layer deposition of SnO_2 for selective room temperature low ppb level O_3 sensing," *ECS Journal of Solid State Science and Technology*, vol. 4, no. 10, pp. S3059–S3061, 2015.

[180] R.-J. Wu, C.-Y. Chen, M.-H. Chen, and Y.-L. Sun, "Photoreduction measurement of ozone using Pt/TiO_2–SnO_2 material at room temperature," *Sensors and Actuators B: Chemical*, vol. 123, no. 2, pp. 1077–1082, 2007.

[181] M. Bender, E. Gagaoudakis, E. Douloufakis et al., "Production and characterization of zinc oxide thin films for room temperature ozone sensing," *Thin Solid Films*, vol. 418, no. 1, pp. 45–50, 2002.

[182] F. S.-S. Chien, C.-R. Wang, Y.-L. Chan, H.-L. Lin, M.-H. Chen, and R.-J. Wu, "Fast-response ozone sensor with ZnO nanorods grown by chemical vapor deposition," *Sensors and Actuators B: Chemical*, vol. 144, no. 1, pp. 120–125, 2010.

[183] M. C. Carotta, A. Cervi, A. Fioravanti et al., "A novel ozone detection at room temperature through UV-LED-assisted ZnO thick film sensors," *Thin Solid Films*, vol. 520, no. 3, pp. 939–946, 2011.

[184] K. L. Chen, G. J. Jiang, K. W. Chang, J. H. Chen, and C. H. Wu, "Gas sensing properties of indium–gallium–zinc–oxide gas sensors in different light intensity," *Analytical Chemistry Research*, vol. 4, pp. 8–12, 2015.

[185] M.-H. Chen, C.-S. Lu, and R.-J. Wu, "Novel Pt/TiO_2–WO_3 materials irradiated by visible light used in a photoreductive ozone sensor," *Journal of the Taiwan Institute of Chemical Engineers*, vol. 45, no. 3, pp. 1043–1048, 2014.

[186] M. Augustin, M. Sommer, and V. V. Sysoev, "UV–VIS sensor system based on SnO_2 nanowires," *Sensors and Actuators A: Physical*, vol. 210, pp. 205–208, 2014.

[187] H. Chen, C. O. Stanier, M. A. Young, and V. H. Grassian, "A kinetic study of ozone decomposition on illuminated oxide surfaces," *Journal of Physical Chemistry A*, vol. 115, no. 43, pp. 11979–11987, 2011.

[188] P. Kofstad, *Non-Stoichiometry, Diffusion and Electrical Conductivity in Binary Metal Oxides*, Wiley, New York, NY, USA, 1972.

[189] M. Căldăraru, D. Sprînceana, V. T. Popa, and N. I. Ionescu, "Surface dynamics in tin dioxide-containing catalysts II. Competition between water and oxygen adsorption on polycrystalline tin dioxide," *Sensors and Actuators B: Chemical*, vol. 30, no. 1, pp. 35–41, 1996.

[190] G. Korotcenkov, V. Brinzari, Y. Boris, M. Ivanov, J. Schwank, and J. Morante, "Influence of surface Pd doping on gas sensing characteristics of SnO_2 thin films deposited by spray pirolysis," *Thin Solid Films*, vol. 436, no. 1, pp. 119–126, 2003.

[191] D. Koziej, N. Bârsan, U. Weimar, J. Szuber, K. Shimanoe, and N. Yamazoe, "Water–oxygen interplay on tin dioxide surface: implication on gas sensing," *Chemical Physics Letters*, vol. 410, no. 4–6, pp. 321–323, 2005.

[192] G. Korotchenkov, V. Brynzari, and S. Dmitriev, "Electrical behavior of SnO_2 thin films in humid atmosphere," *Sensors and Actuators B: Chemical*, vol. 54, no. 3, pp. 197–201, 1999.

[193] V. E. Henrich and P. A. Cox, *The Surface Science of Metal Oxides*, Cambridge University Press, New York, NY, USA, 1994.

[194] A. R. Gonzalez-Elipe, G. Munuera, and J. Soria, "Photo-adsorption and photo-desorption of oxygen on highly hydroxylated TiO_2 surfaces. Part 2.—study of radical intermediates by electron paramagnetic resonance," *Journal of the Chemical Society, Faraday Transactions 1: Physical Chemistry in Condensed Phases*, vol. 75, pp. 748–761, 1979.

[195] C. Sivadinarayana, T. V. Choudhary, L. L. Daemen, J. Eckert, and D. W. Goodman, "The nature of the surface species formed on Au/TiO_2 during the reaction of H_2 and O_2: an inelastic neutron scattering study," *Journal of the American Chemical Society*, vol. 126, no. 1, pp. 38–39, 2004.

[196] M. Addamo, V. Augugliaro, E. García-López, V. Loddo, G. Marcì, and L. Palmisano, "Oxidation of oxalate ion in aqueous suspensions of TiO_2 by photocatalysis and ozonation," *Catalysis Today*, vol. 107-108, pp. 612–618, 2005.

[197] M. Egashira, M. Nakashima, S. Kawasumi, and T. Selyama, "Temperature programmed desorption study of water adsorbed on metal oxides. 2. Tin oxide surface," *The Journal of Physical Chemistry*, vol. 85, pp. 4125–4130, 1981.

[198] V. A. Gercher and D. F. Cox, "Water adsorption on stoichiometric and defective $SnO_2(110)$ surfaces," *Surface Science*, vol. 322, no. 1–3, pp. 177–184, 1995.

[199] E. Leblanc, L. Perier-Camby, G. Thomas, R. Gibert, M. Primet, and P. Gelin, "NO_x adsorption onto dehydroxylated or hydroxylated tin dioxide surface. Application to SnO_2-based sensors," *Sensors and Actuators B: Chemical*, vol. 62, no. 1, pp. 67–72, 2000.

[200] M. Z. Atashbar, B. Gong, H. T. Sun, W. Wlodarski, and R. Lamb, "Investigation on ozone-sensitive In_2O_3 thin films," *Thin Solid Films*, vol. 354, no. 1, pp. 222–226, 1999.

[201] J. W. Gardner, "A non-linear diffusion-reaction model of electrical conduction in semiconductor gas sensors," *Sensors and Actuators B: Chemical*, vol. 1, no. 1–6, pp. 166–170, 1990.

[202] D. E. Williams, G. S. Henshaw, K. F. E. Pratt, and R. Peat, "Reaction-diffusion effects and systematic design of gas-sensitive resistors based on semiconducting oxides," *Journal of the Chemical Society, Faraday Transactions*, vol. 91, no. 23, pp. 4299–4307, 1995.

[203] D. E. Williams and K. F. E. Pratt, "Theory of self-diagnostic sensor array devices using gas-sensitive resistors," *Journal of the Chemical Society, Faraday Transactions*, vol. 91, no. 13, pp. 1961–1966, 1995.

[204] H. Lu, W. Ma, J. Gao, and J. Li, "Diffusion-reaction theory for conductance response in metal oxide gas sensing thin films," *Sensors and Actuators B: Chemical*, vol. 66, no. 1, pp. 228–231, 2000.

[205] X. Vilanova, E. Llobet, R. Alcubilla, J. E. Sueiras, and X. Correig, "Analysis of the conductance transient in thick-film tin oxide gas sensors," *Sensors and Actuators B: Chemical*, vol. 31, no. 3, pp. 175–180, 1996.

[206] G. Sakai, N. Matsunaga, K. Shimanoe, and N. Yamazoe, "Theory of gas-diffusion controlled sensitivity for thin film semiconductor gas sensor," *Sensors and Actuators B: Chemical*, vol. 80, no. 2, pp. 125–131, 2001.

[207] S. Nakata, K. Takemura, and K. Neya, "Non-linear dynamic responses of a semiconductor gas sensor: evaluation of kinetic parameters and competition effect on the sensor response," *Sensors and Actuators B: Chemical*, vol. 76, no. 1–3, pp. 436–441, 2001.

[208] E. Llobet, X. Vilanova, J. Brezmes, J. E. Sueiras, R. Alcubilla, and X. Correig, "Steady-state and transient behavior of thick-film tin oxide sensors in the presence of gas mixtures," *Journal of the Electrochemical Society*, vol. 145, no. 5, pp. 1772–1779, 1998.

[209] W. Zhixiang, M. Fenzhu, S. Yiqiang, Z. Ming, and Y. Guocong, "A method for the measurement of gas concentration distribution in the adsorptive bed," *Chemical Engineering Science*, vol. 54, no. 23, pp. 5755–5760, 1999.

[210] Y. Shimizu, T. Maekawa, Y. Nakamura, and M. Egashira, "Effects of gas diffusivity and reactivity on sensing properties of thick film SnO_2-based sensors," *Sensors and Actuators B: Chemical*, vol. 46, no. 3, pp. 163–168, 1998.

[211] G. Korotchenkov, V. Brynzari, and S. Dmitriev, "Kinetics characteristics of SnO_2 thin film gas sensors for environmental monitoring," in *Chemical Microsensors and Applications*, S. Buettgenbach, Ed., vol. 3539 of *Proceedings of SPIE*, pp. 196–204, December 1998.

[212] V. Brynzari, G. Korotchenkov, and S. Dmitriev, "Simulation of thin film gas sensors kinetics," *Sensors and Actuators B: Chemical*, vol. 61, no. 1, pp. 143–153, 1999.

[213] A. Šetkus, "Heterogeneous reaction rate based description of the response kinetics in metal oxide gas sensors," *Sensors and Actuators B: Chemical*, vol. 87, no. 2, pp. 346–357, 2002.

[214] V. P. Zhdanov, "Impact of surface science on the understanding of kinetics of heterogeneous catalytic reactions," *Surface Science*, vol. 500, pp. 965–984, 2002.

[215] H. J. Kreuzer, "Theory of surface processes," *Applied Physics A*, vol. 51, no. 6, pp. 491–497, 1990.

[216] C. Xu and B. E. Koel, "Adsorption kinetics on chemically modified or bimetallic surfaces," *The Journal of Chemical Physics*, vol. 100, no. 1, pp. 664–670, 1994.

[217] U. Brossmann, U. Södervall, R. Würschum, and H. Schaefer, " ^{18}O Diffusion in nano crystalline ZrO_2," *Nanostructured Materials*, vol. 12, no. 5–8, pp. 871–874, 1999.

[218] Y. Ikuma and T. Murakami, "Oxygen tracer diffusion in polycrystalline In_2O_3," *Journal of the Electrochemical Society*, vol. 143, no. 8, pp. 2698–2702, 1996.

[219] H. Yamaura, T. Jinkawa, J. Tamaki, K. Moriya, N. Miura, and N. Yamazoe, "Indium oxide-based gas sensor for selective detection of CO," *Sensors and Actuators B: Chemical*, vol. 36, no. 1–3, pp. 325–332, 1996.

[220] M. Haneda, Y. Kintaichi, N. Bion, and H. Hamada, "Mechanistic study of the effect of coexisting H_2O on the selective reduction of NO with propene over sol-gel prepared In_2O_3-Al_2O_3 catalyst," *Applied Catalysis B: Environmental*, vol. 42, no. 1, pp. 57–68, 2003.

[221] J. Berger, I. Riess, and D. S. Tannhauser, "Dynamic measurement of oxygen diffusion in indium-tin oxide," *Solid State Ionics*, vol. 15, no. 3, pp. 225–231, 1985.

[222] C. N. Satterfield, *Mass Transfer in Heterogeneous Catalysis*, MIT Press, Cambridge, Mass, USA, 1970.

[223] N. Matsunaga, G. Sakai, K. Shimanoe, and N. Yamazoe, "Formulation of gas diffusion dynamics for thin film semiconductor gas sensor based on simple reaction–diffusion equation," *Sensors and Actuators B: Chemical*, vol. 96, no. 1-2, pp. 226–233, 2003.

[224] J. R. Stetter, "A surface chemical view of gas detection," *Journal of Colloid And Interface Science*, vol. 65, no. 3, pp. 432–443, 1978.